Copyright © 1996, by the author(s).
All rights reserved.

Permission to make digital or hard copies of all or part of this work for personal or classroom use is granted without fee provided that copies are not made or distributed for profit or commercial advantage and that copies bear this notice and the full citation on the first page. To copy otherwise, to republish, to post on servers or to redistribute to lists, requires prior specific permission.

ETCHING FOR MICROMACHINING PROCESSING

by

Kirt R. Williams and Richard S. Muller

Memorandum No. UCB/ERL M96/37

18 June 1996

(Revised 29 July 1996)

COVER PAGE

ETCHING FOR MICROMACHINING PROCESSING

by

Kirt R. Williams and Richard S. Muller

Memorandum No. UCB/ERL M96/37

18 June 1996

(Revised 29 July 1996)

ELECTRONICS RESEARCH LABORATORY

College of Engineering
University of California, Berkeley
94720

Etching for Micromachining Processing

Kirt R. Williams and Richard S. Muller

Berkeley Sensor & Actuator Center
University of California at Berkeley
497 Cory Hall
Berkeley, CA 94720-1770

18 June 1996
(minor corrections 29 July 1996)

Abstract

The etch rates for 317 combinations of 16 materials (single-crystal silicon, doped and undoped polysilicon, several types of silicon oxide, stoichiometric and silicon-rich silicon nitride, aluminum, tungsten, titanium, Ti/W alloy, and two brands of positive photoresist) used in the fabrication of microelectromechanical systems and integrated circuits in 28 wet, plasma, and plasmaless-gas-phase etches (several HF solutions, H_3PO_4, $HNO_3 + H_2O + NH_4F$, KOH, Type A aluminum etchant, $H_2O + H_2O_2 + HF$, H_2O_2, piranha, acetone, HF vapor, XeF_2, and various combinations of SF_6, CF_4, CHF_3, Cl_2, O_2, N_2, and He in plasmas) were measured and are tabulated. Etch preparation, use, and chemical reactions (from the technical literature) are given. Sample preparation and MEMS applications are described for the materials.

Because etch rates vary with a number of conditions, we also report in the tables the observed range of etch rates by the authors and others in our laboratory. To help explain this variation, we discuss at the length the chemical and physical steps in wet and dry etching, leading up to discussions of 15 sources of wet-etch-rate variation and 14 sources of plasma-etch-rate variation.

Tips on determining when an etch is complete are given.

Contents

Table of Figures

Table of Tables

I. INTRODUCTION

When designing a new process flow for fabricating micromachined devices, the etch rate of each layer that is to be patterned must be known. While the etch rates of many etchants that target specific materials (e.g., thermally grown silicon dioxide in 5:1 buffered hydrofluoric acid) are commonly known, the etch rates of the masking and underlying films are frequently not available in the literature. This paper provides this information for 317 different combinations of 16 materials and 28 etches used in the micromachining of microelectromechanical systems (MEMS) and in integrated-circuit processing. These etch-rate data, based on tests performed in the U. C. Berkeley Microfabrication Laboratory (Berkeley Microlab), are provided in table form.

Recognizing that etch rates vary due to many process factors (e.g., previous use of solution or plasma chamber, temperature, area of wafer exposed), we have included further data in the tables on the observed range of etch rates to provide an idea of the range of etch rates that might be expected. These data are obtained from the authors and others in our laboratory. Because etches are normally not perfectly reproducible, we discuss at length the physical and chemical steps in wet and plasma etches and sources of etch-rate variation, giving reactions and variations with parameters such as temperature and concentration, if these are known from the literature on etching. We also give methods of reducing some types of variation.

In addition to the tables and variation information, this paper describes the measurement techniques used, the sample preparation and MEMS applications for each the materials, the preparation and use of each etch, and tips on end-of-etch detection.

II. WET-ETCH PROCESSES AND ETCH-RATE VARIATION

A. *Overview of Wet Etches*

Most wet etches use water as the solvent for a chemical or chemicals, typically acids or bases, which react chemically with the target material. Wafers are placed singly in holders or in groups in cassettes, which hold the wafers during wet-etch and rinse steps.

B. *Wet-Etch Processes*

A review of the physical and chemical processes involved in etching is required for a discussion of what causes etch rates to vary and how to achieve a uniform, repeatable etch. In any etch, reactants must (Fig. 1) (*a*) be formed in the bulk solution; (*b*) be transported to the etch site, which requires the substeps of mixing (forced or convective) or diffusion through a transition layer in the liquid to the vicinity of the surface, diffusion through a stagnant boundary layer to the surface, adsorption onto the surface, and diffusion along the surface to the etch site; (*c*) react, which often involves a complicated series of oxidation-reduction subreactions that may take place at pairs of highly localized adjacent sites; and (*d*) etch products must leave the site, which again may require diffusion along a surface and desorption and diffusion through a boundary layer.

The rate of each step can be expressed in terms of fluxes (particles per unit area per unit time) of chemicals for a balanced reaction being generated, transported to, consumed by, and transported from the etch site. The slowest of the above steps is the rate-limiting step, which determines the etch rate at a particular location on a wafer. In steady-state, all steps following the rate-limiting step will be effectively controlled by the rate of this step. If the rates of two

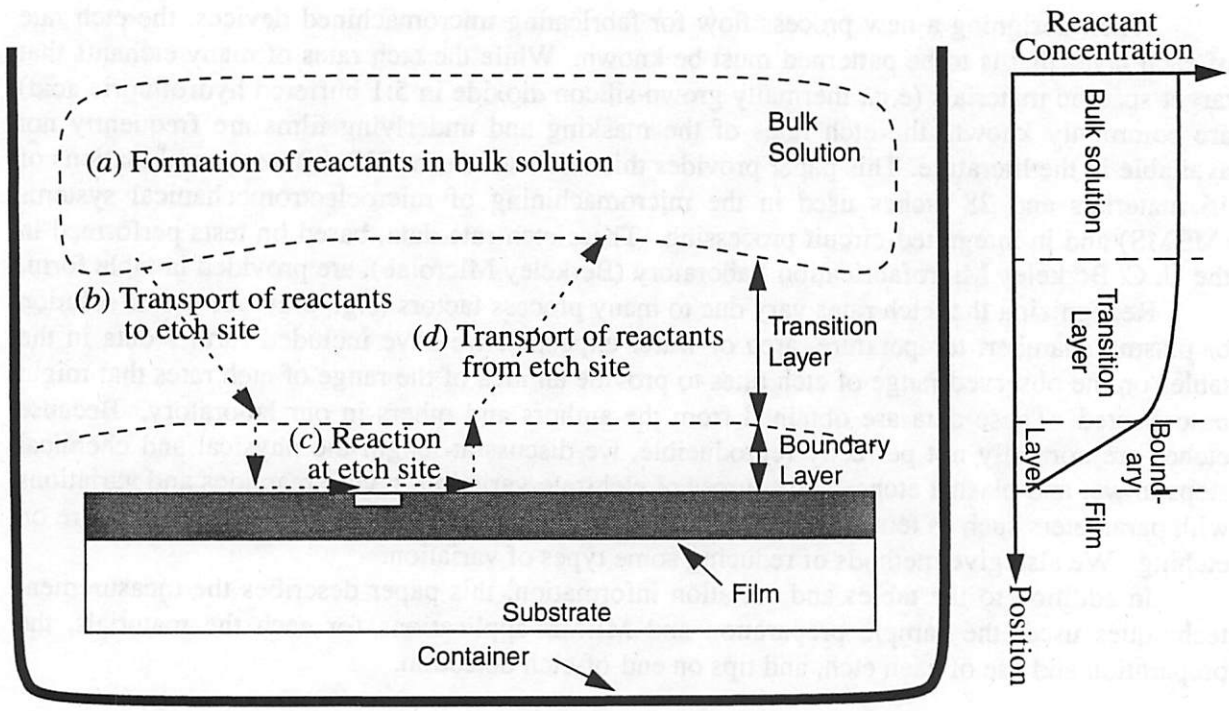

Figure 1 Chemical and physical steps in the wet-etch process.

steps are of the same order of magnitude, both affect the etch rate, reducing it to less than the slower of the two. This can be modeled using a Deal-Grove-type model [1,2].

The following approximations for each of the four steps described above will aid in the discussion of etch-rate variation.

(*a*) (*i*) *Formation of etch reactants in the bulk solution--equilibrium concentrations*: The dissociation constants for weak acids and bases, K_a and K_b, are used to find the equilibrium values of ion concentrations using the law of mass action. For acids, the equation is

$$K_a(T) = \frac{[H^+][An^-]}{[HAn]} \tag{1}$$

where $[H^+]$ is the hydrogen ion concentration, $[An^-]$ is the concentration of some anion, and [HAn] is the concentration of associated acid molecules. K_a and K_b are Arrhenius functions of temperature, according to the form

$$K_a = K_{a0}e^{-E_{Aa}/kT} \tag{2}$$

where K_{a0} is a constant. Thus, in *equilibrium* at higher temperatures, more H^+ ions ANd anions and less associated molecules are available for a given reaction. The actual supply, however, also depends on the *generation rate* of reactants, as discussed below.

(*a*) (*ii*) *Formation of etch reactants in the bulk solution--generation rates*: In many cases, such as the dissociation of strong acids at lower concentrations, all of the reactive species are formed when the solution is mixed. In other cases, however (e.g., HF solutions), only a limited quantity of the active species is formed upon mixing. As these species are consumed, more are generated through reactions in the bulk solution. The reaction rate RR of most such chemical reactions follow Arrhenius equations of the type

$$RR = K_1 n_1 e^{-E_{A1}/kT} \tag{3}$$

or

$$RR = K_2 n_1 n_2 e^{-E_{A2}/kT} \tag{4}$$

for one- or two-species reactions, respectively, where K_1 and K_2 are pre-exponential frequency factors, n_1 and n_2 are the concentrations (cm^{-3}) of species 1 and 2, E_{A1} and E_{A2} are the activation energies for the reactions, k is the Boltzmann constant, and T is the absolute temperature.

For a combination of sufficiently slow etch and rapid generation rates, the supply concentration throughout the bulk solution will be near equilibrium and constant. If the relative rates are reversed, the overall etch rate may be slowed by a lower-than-equilibrium supply concentration.

(*b*) (*i*) *Mixing transport in a liquid*: Reactants moving from the bulk solution to the etch surface pass through a region of lower concentration than that in the bulk. This region can be divided into the boundary layer near the etch surface, which is mostly stagnant, and the transition layer, which is between the boundary layer and the bulk solution (Fig. 1) [3]. The boundaries of these layers are not well defined and vary with position on the wafer.

The transport of chemicals through the transition layer is due to both diffusion and mixing. Mixing, either forced (by agitation) or via convection (due to thermal or density gradients) thins the transition layer and raises its concentration profile closer to that in the bulk solution. The concentration at the edges of the boundary layer therefore rises, increasing the diffusive flux that is possible, as discussed below. Mixing can also thin the boundary layer. These raise the etch rate if diffusion is the rate-limiting step.

(*b*) (*ii*) *Diffusive transport in a liquid to the etch site*: Reactants flow through the boundary layer via diffusion. The diffusive flux Γ of a species in steady state, assuming no gain or loss of the diffusing species, is given by

$$\Gamma = -D\frac{dn}{dx} = D\frac{n_{bound}-n_{surf}}{\delta} \quad , \tag{5}$$

where D is the diffusivity, $dn/dx = (n_{bound}-n_{surf})/\delta$ is the concentration gradient, n_{bound} and n_{surf} are the concentrations (in particles per unit volume) of the species at the edge of the boundary layer and at the surface, and δ is the thickness of the boundary layer, which contains slow-moving and stagnant fluid. The boundary-layer thickness varies with $1/\sqrt{v}$, where v is the free-flow fluid velocity outside the boundary layer [1,3]. The boundary-layer thickness also varies with location on a wafer, becoming wider downstream from protrusions on the surface.

The diffusivity of a species in a liquid is similar to that in a solid, typically varying with temperature as the Arrhenius-factor function

$$D = AT^{1/2}e^{-E_{Ad}/kT} \quad , \tag{6}$$

where A is a constant and E_{Ad} is the activation energy for diffusion [4]. The diffusivity can rise or fall with concentration, depending on the species involved.

The surface diffusivity also follows an Arrhenius-type equation.

Increasing the flux by raising the diffusivity or boundary-layer-edge concentration, or by reducing the boundary-layer thickness or surface concentration, will enhance the etch rate, if this is the rate-limiting step.

(*c*) *Surface-reaction rate*: The surface-reaction rate SR varies as

$$SR = K_s e^{-E_{As}/kT} n' \tag{7}$$

where K_s is the surface-reaction-rate prefactor, E_{As} is the surface-reaction activation energy, and n' is the surface concentration (in particles per unit area).

The rate-limiting step can, in some cases, be altered. For example, at low concentrations, the etch may be mass-transfer-limited, but can become surface-reaction-rate limited at higher concentrations or with agitation, both of which increase the supply of reactants to the reaction site. As another example, an etch that is limited by the surface-reaction rate may be sped up by heating, eventually becoming mass-transfer-limited.

(*d*) *Diffusive transport in a liquid away from the etch site*: Diffusive transport of products from the etch site is analogous to the diffusion of reactants to the etch site (except that the relevant flux is away from the surface), as discussed in Section (*b*).

C. *Wet-Etch-Rate Variation*

The sources of etch-rate variation can be divided into three categories: the etch setup, the material being etched, and the layout and structure on the substrate. The most significant effects on wet-etch rate in each category are as follows.

Etch-rate variation due to the etch setup is a function of (*i*) temperature, (*ii*) loss of reactive species, (*iii*) loss of liquids to evaporation, (*iv*) mixing, (*v*) stratification of the solution, (*vi*) etch-product blocking of chemical flow, (*vii*) elapsed time from the start of the etch, (*viii*) applied potential, (*ix*) illumination, and (*x*) contamination. Etch-rate variation due to the material being etched is affected by (*xi*) impurities in or on the material being etched, (*xii*) microstructure, and (*xiii*) film stress. Etch-rate variation due the layout and structure on the substrate is affected by (*xiv*) the distribution and fraction of surface area of the target layer exposed

and (*xv*) the structure geometry.

The manner in which the etch rate varies with each of these variables (some of which can be controlled, as summarized in Table 1) is discussed below. There are probably still other factors that affect etch rates not listed here.

(*i*) *Temperature*: Increasing temperature increases the etch rate of surface-reaction- and supply-limited reactions by speeding up surface reactions (Eq. 7) and by increasing the equilibrium concentrations of reactive species in the solution (for solutions involving partially dissociated compounds, Eqs. 2 and 3). In many such cases (non-diffusion-limited etching in hydrofluoric acid, phosphoric acid, or potassium hydroxide) the etch rate ER is described by

$$ER = A_a e^{-E_{Aa}/kT} \tag{8}$$

where A_a is a constant and E_{Aa} is the apparent activation energy. Apparent activation energy takes into account the effects of temperature on both supply of reactive species and the reaction itself. Since the bulk concentration may rise and the diffusivity does rise with temperature (Eq. 6), diffusion-limited etching is also enhanced by raising the temperature.

Temperature-controlled baths can reduce temperature variation. If local heating occurs because of a strongly exothermic reaction, agitation helps to maintain a constant temperature through the volume of the solution.

(*ii*) *Loss of reactive species*: Previous use of a solution often results in a reduced etch rate due to depletion of a reactive species. Using a larger volume of etchant and buffering (e.g., 5:1 BHF) both act to reduce this effect. Use of fresh solutions for each batch of wafers also reduces etch-rate variation, although noticeable depletion may still occur during long etches. Spray etches, which supply streams of fresh solution, are an alternative to etch baths.

(*iii*) *Loss of liquids to evaporation*: Water and other chemicals can be lost to evaporation. Evaporation of water increases the concentration of a solution. In most cases, the increased concentration raises the etch rate, but in others, such as that of silicon nitride in 85% phosphoric acid and of silicon in 33% potassium hydroxide, the etch rates go down. This rate reduction may be due to water playing a role in the creation of reactive species (e.g., dissociation of an acid) or because water is involved in the reaction itself (as is the case for KOH etching of Si [5,6]). The use of a reflux system (which condenses vapor and returns the liquid to the solution) helps keep the water concentration, and thus the etch rate, constant.

Other chemicals with high vapor pressures can also evaporate to change the concentration. HF will evaporate faster than H_2O in mixtures greater than about 35% HF (the azeotropic concentration), making the solution etch oxides more slowly. Storing the solution covered will reduce this effect.

Although loss of chemicals is similar to the loss of reactive species (listed in (*ii*) above), it takes place mainly through evaporation rather than through exhaustion by chemical reaction, and can occur even when the solution is not in use.

(*iv*) *Mixing*: Mixing, whether forced or occurring without intervention (e.g., due to self heating), can accelerate etching in several ways. First, mixing increases the frequency of collisions of reactants, slightly raising the frequency factors K_1 and K_2 in Eqs. 4 and 5, increasing the production rate of reactants.

Mixing has the most significant effect on diffusion-limited etching by decreasing the transition-layer thickness and the boundary-layer thickness δ (Eq. 5). This holds whether turbulent or laminar flow occurs.

(*v*) *Stratification of the solution*: Some etchants, such as KOH, have been observed to stratify, causing an etch-rate gradient from the top to the bottom of the bath. To prevent such a

Wet-Etch-Rate Variation				
User-Controlled Parameter	Limiting Step in the Etch	Pertinent Equation(s)	Approximate Effect	Explanation/ Assumptions
Temperature	Generation of reactants in bulk solution	$RR = K_1 n_1 n_2 e^{-E_{A1}/kT}$ $K_a = K_0 e^{-E_{Aa}/kT}$	$ER \propto e^{-E_A/kT}$	Temperature will affect both reaction rates and dissociation constants. assumes reactants are used immediately. (influence of diffusion is negligible).
	Diffusive transport through a boundary layer	$\Gamma = -D(n_{bound} - n_{surf})/\delta$ $D = AT^{1/2} e^{-E_{AD}/kT}$	$ER \propto T^{1/2} e^{-E_A/kT}$	Assumes boundary and surface concs. are constant. Both may vary with T.
	Reaction rate at surface	$SR = K_s e^{-E_{AS}/kT} n'$	$ER \propto e^{-E_A/kT}$	Assumes areal surf. conc. n' is constant. It will vary with SR and Γ, and thus T.
Mixing	Generation of reactants	$RR = K_1 n_1 n_2 e^{-E_{A1}/kT}$	0 or $ER \uparrow$	The frequency prefactor rises slightly.
	Diffusive transport through a boundary layer	$\Gamma = -D(n_{bound} - n_{surf})/\delta$	$ER \uparrow$	Supply conc. rises and boundary layer δ gets thinner.
	Reaction rate at surface	$SR = K_s e^{-E_{AS}/kT} n'$	$ER \uparrow$	The surface concentration of reactants n' rises.
Fresh Solution	Generation of reactants in bulk solution	$RR = K_1 n_1 e^{-E_{A1}/kT}$ $RR = K_2 n_1 n_2 e^{-E_{A1}/kT}$	$ER \uparrow$	More reactants n_1 and n_2 are available.
	Diffusive transport through a boundary layer	$\Gamma = -D(n_{bound} - n_{surf})/\delta$	$ER \uparrow$	The bulk conc. and boundary conc. n_{bound} rise.
	Reaction rate at surface	$SR = K_s e^{-E_{AS}/kT} n'$	$ER \uparrow$	The areal surface concentration of reactants n' probably rises.

Table 1 User-controllable parameters in wet-etch-rate variation

gradient, a recirculating pump for the KOH bath is used in the Berkeley Microlab.

(*vi*) *Etch-product blocking of chemical flow*: The flow of reactants to, and of products from, a surface can be blocked by etch products, such as gas bubbles (e.g., during aluminum etching in Type A aluminum etchant), or by a passivating layer that masks the area being etched. This can slow the etch locally or across the whole wafer. The removal of gas bubbles can be aided by agitation or the addition of a surfactant (e.g., alkylaryl polyether alcohol, produced commercially as Baker Triton X-100).

A passivating layer can be caused by adsorbed nonreactive species or the growth of an epitaxial film such as an oxide film [7]. In many cases, another chemical can be added to the etchant that targets the passivating layer (e.g., the HF created in the silicon wet etchant removes the silicon oxide formed during an intermediate step).

(*vii*) *Elapsed time from the start of an etch*: Elapsed time from the start of an etch can affect the average etch rate in two ways. First, if mass transport is the rate-limiting step, at the beginning of the etch (before steady-state etching conditions are reached), the supply of reactants near the surface is more plentiful, so the etch rate is higher.

Second, some etchants, particularly those with high surface tension, require time to wet small features on a surface completely, which decreases the effective etch rate. Prewetting a wafer by dipping it in water before placing it in the etchant or adding a surfactant to the etchant accelerates wetting and thus the initiation of etching in all locations, improving the etch uniformity between large and small features.

In both cases, two 10-second etches yield different average etch rates than does a single 20-second etch; the direction will depend on which of the above two effects dominates.

(*viii*) *Applied potential*: Since many of the steps in an etch are electrochemical, and since ions are frequently involved, an applied potential should be expected to affect both the flow of ions to and from an etch front and the etch reaction itself. An applied potential can be produced externally, by an outside voltage source, or generated "internally" in the etch bath, as with a photovoltaically or electrochemically created potential.

An example of an externally applied potential is that used to create porous silicon, in which a silicon wafer (of any type and doping) is biased positively with respect to a hydrofluoric acid solution [2,8]. At zero potential, no etching of the silicon occurs. With a sufficiently large positive bias, the silicon is oxidized and etched away (a larger bias is required for more heavily doped *n*-type silicon). Variations in the voltage cause variations in the etch rate.

A potential difference can be created within the etch bath by electrically connected materials with different work functions, such as a *p*-*n* junction. A silicon selective-staining technique in a HF-HNO_3 solution exploits this potential to etch silicon from the *p*-type regions but not from the *n*-type regions [2,9].

A potential difference can also inhibit a desired reaction. This has been observed in the BHF etching of a thin layer of silicon dioxide above the *n* side of a p^+-n^+ junction while under illumination with ambient light [10]. The generated photovoltage biases the p^+ side (and BHF) positive with respect to the n^+ side of the junction, creating an electric field across the oxide that completely stops etching. An externally applied potential has the same effect, with thicker residual oxide layers remaining for larger voltages [10].

(*ix*) *Illumination*: In addition to the photovoltaic effect discussed above, illumination of a semiconductor with sufficiently energetic photons creates electron-hole pairs, which may allow the conduction of electron or hole current needed for a reaction at the surface of a semiconductor, greatly enhancing the etch rate. An example of this is the anodic etching of *n*-type silicon in HF to create porous silicon. Illumination creates holes, which drift to the etch surface and take

part in the reaction, increasing the etch rate [2,11].

(*x*) *Contamination*: As there are many possible types of contamination, it is difficult to predict all effects of contamination. Possible consequences include unexpected etching from a residual chemical left in a poorly rinsed etching tank, faster etching due to an additional reaction taking place or due to catalysis, or slower etching caused by consumption of the etching species or by the formation of a new etch product that blocks the flow of fresh chemicals.

(*xi*) *Impurities in or on the material being etched*: Impurities in the material under etch, whether intentional (e.g., doping) or not, can affect the etch rate. In some cases, a few molar percent of impurity changes the etch rate by more than an order of magnitude (e.g., phosphosilicate glass (PSG) is etched about 14 times faster than low-temperature oxide (LTO) in 10:1 HF). If the additional component is etched relatively very slowly, it can be viewed as blocking a fraction of the surface area, thus slowing the etch in proportion to its concentration (e.g, tungsten cosputtered with titanium, etched in H_2O_2). Conversely, if the additive is etched relatively rapidly, a porous version of the pure material is left at the surface, and etching is sped up (e.g., P_2O_5 in low-pressure chemical-vapor deposited (LPCVD) SiO_2, and argon incorporated in sputtered oxide [12]).

In silicon, the Fermi level is affected by doping, which affects the supply of electrons at the surface of the silicon where the reaction takes place. A few tenths of a percent of boron doping can stop the etching of single-crystal silicon in hydroxide [13] and ethylenediamine-pyrocatechol (EDP) [14] solutions.

Thin films unintentionally *on* the target layer can block the flow of etchants, slowing or stopping etching until removed. Examples are native oxides, which can form when metals and silicon are exposed to room air, and undeveloped photoresist residue.

(*xii*) *Microstructure*: By microstructure, we mean such properties as grain size and orientation, porosity, and crystal defects. All of these properties can affect the etch rate. Many films (e.g. polysilicon) have preferred grain orientations, and some crystal faces etch faster than others in some etchants. Film microstructures vary with deposition conditions and subsequent heat treatments (e.g., annealing PSG), and can vary through the thickness of a film (e.g., LPCVD polysilicon [15]). Defects can be caused during processing.

Smaller grains tend to etch more rapidly, as grain boundaries are higher-energy regions from which atoms are more easily removed [16,17]. Dislocations are likewise crystal regions of high energy, so high-dislocation-density films should be expected to etch faster [16]. More-porous films also etch more rapidly, as etchants can penetrate the film more easily and there is less material per unit volume to be removed [17]. The porosity of some films (e.g., LTO) can be decreased by annealing.

(*xiii*) *Film stress*: Residual stress in a material can affect its etch rate. For example, both single-crystal silicon in KOH [18] and silicon dioxide in BHF [19] are etched more rapidly in tension than under compression. A reason for this relationship has not been presented in the literature, but it can be theorized that in tension, the atoms in a solid are pulled from their quiescent positions relative to each other. Some of the energy required to remove them has thus been supplied mechanically, so that less chemical energy is required to break the bonds in the solid. The opposite can be argued for solids under compression.

The stress state may, however, be less significant than other parameters, such as porosity and incorporation of other materials into the film [12]. Variation in residual stress can be caused by different deposition and annealing conditions, by the use of substrates with different thermal expansion rates, and even by masking layers [17].

(*xiv*) *Distribution and fraction of surface area of the target layer exposed*: Distribution and fraction of surface area of the target layer exposed is important if the reaction is limited by the transport of reactants to the etch site. The etch rate can be slower in the locations of a wafer with the highest demand (largest areas of film being etched) and that are farthest from the bulk solution (e.g., the center of the wafer or between wafers in a cassette). (This is referred to as "loading.") For this reason, the wet-etch rates for the 100%-exposure-area wafers in Table 3 can be considered to be a lower limit. Agitation to keep the concentration of reactants uniform reduces this effect.

Uniformity of etching is also promoted by making the features to be etched of small size and the windows in the mask of uniform shape, and by placing them far apart, so that each has the same demand for reactants and the etchant consumption in one region does not interfere with that of its neighbors. Lowering the reaction rate at the surface (e.g., by lowering the temperature) permits a sufficient supply of reactants to reach the reaction site and favors uniformity (assuming that the diffusivity does not drop dramatically).

(*xv*) *Structure geometry*: Small depth variations in the surface topography, (smaller than the boundary-layer thickness), have little or no effect on etch rates. Deep-aspect-ratio trenches (i.e., much deeper than they are wide) and structures requiring a lot of undercut are etched more slowly (aperture effect). For sufficiently long transport paths, etches are limited by the diffusion of reactants to or of products from the etch site (Eq. 5).

III. PLASMA-ETCH PROCESSES AND ETCH-RATE VARIATION

A. *Overview of Plasma Etches*

The plasmas used for etching are gases composed of a neutral feed gas and dissociated molecules along with a small concentration of ions and electrons. The bulk of the plasma, which is most of the volume of the plasma chamber away from the walls, contains equal numbers of positively and negatively charged species, and is therefore electrically neutral. Between the edges of the bulk plasma and the plasma chamber walls are the sheaths, which are high-electric-field regions with the field pointing away from the bulk plasma (Fig. 2). The bulk plasma is therefore positive with respect to the walls.

The sheaths drive the positive ions that enter them outward to the walls, while containing electrons for most of the AC drive cycle. The voltage drop through the sheaths varies from around zero to a large positive value during the cycle. Because the bulk plasma has no voltage drop across it, the difference between the sheath voltages is equal to the drive voltage. The sheath voltages increase with increasing plasma-generation input power and decreasing electrode area.

The most common plasma-etching systems used for micromachining are parallel-plate reactors (Fig. 2). Energy is supplied to the plasma from a capacitively coupled radio-frequency (typically 13.56 MHz) power supply. The RF field accelerates the low-mass electrons to energies averaging a few electron volts, while the ions are too massive to respond to such high-frequency fields. The electrons continuously pass energy to gas molecules through inelastic collisions, creating radicals, ions, and more electrons. (The term "radical" is used in plasma physics for atoms or groups of atoms that are electrically neutral, but have incomplete chemical bonding, making them very reactive. Examples are Cl and CF_3.) Kinetic energy of ions and neutrals is lost to the walls and exhaust as energetic particles leave the system. Typical operating pressures

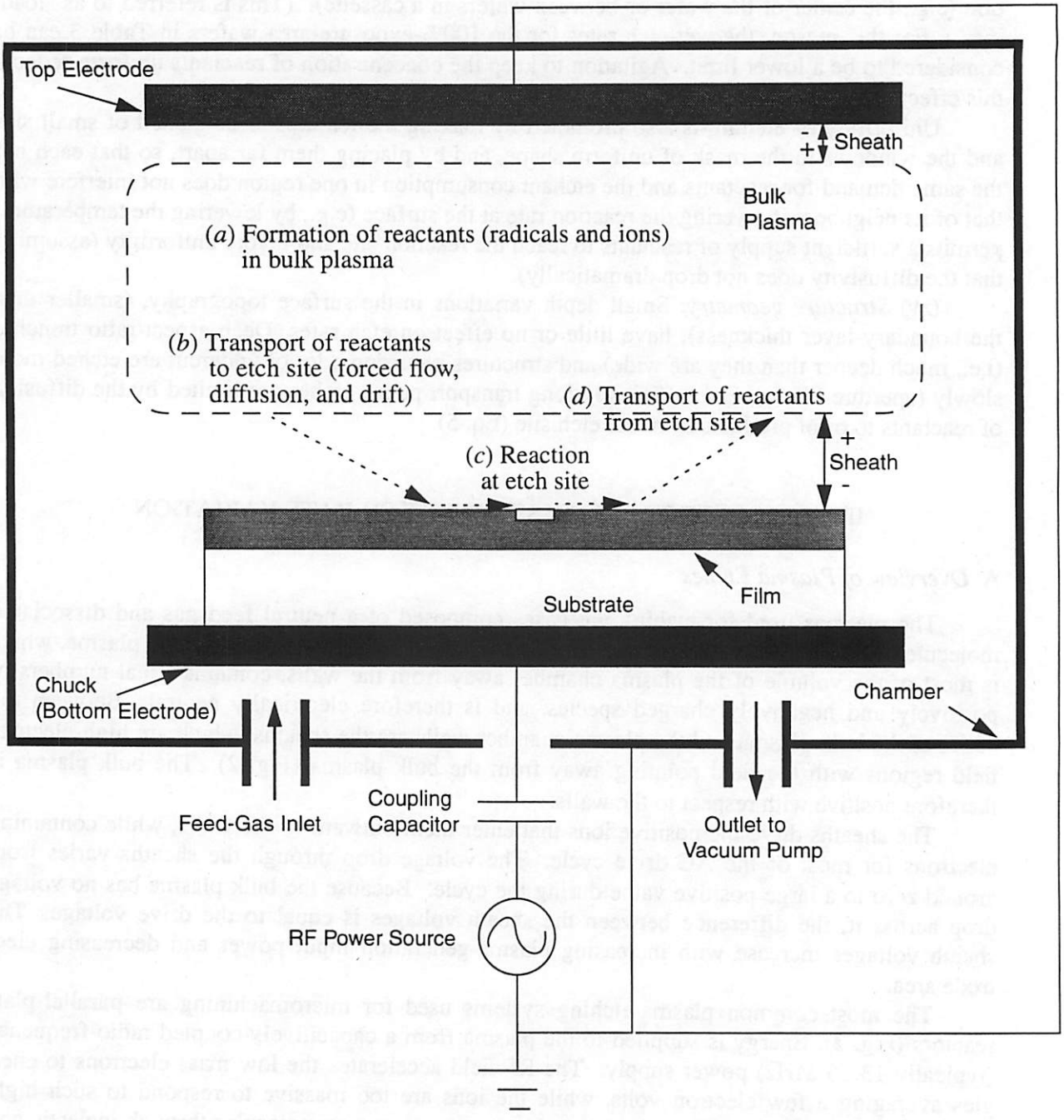

Figure 2 Parallel-plate reactor--physical and chemical steps in the plasma-etch process.

are 0.01 to 10 Torr [17], and with the fraction of ionized species being 10^{-4} to 10^{-6} [20], electron densities (also known as plasma densities) are in the range 10^9 to 10^{12} cm^{-3} [20,21]. The density of radicals increases with power, normally being 5 to 50% of the total number of neutrals [20].

Plasma etches can be divided into three classes, depending on the degree of ion-bombardment involvement in the etch: chemical-plasma etching, ion-enhanced etching, and sputtering.

Chemical-plasma etching (usually referred to simply as "plasma etching") is purely chemical: chemically active neutrals (mostly radicals, but also stable gas molecules), are generated from the input gases in the source plasma, then travel out of the bulk plasma to the wafer surface, where they are responsible for all of the etching that occurs. The sheath voltages in chemical-plasma etching are relatively low (tens of volts) [1] and the pressures are moderate to high (in the 300-mTorr range). With the resulting shorter mean-free paths and low electric fields, ions cannot gain sufficient energy as they traverse the sheath to affect the etch. Purely chemical plasma etching is fairly isotropic: the reactive gas neutrals move via diffusion and mixing just as do the reactive species in a liquid, and can therefore undercut masking layers (Fig. 3). Halogen-containing feed gases are used for most plasma etches (an exception is the purely oxygen-based plasmas used to etch photoresist).

Ion-enhanced etching is usually done at the same or at slightly lower pressures than purely chemical plasma etching (a typical value in the Berkeley Microlab is 250 mTorr, although overlap of the pressure ranges occurs) and with a larger voltage drop (hundreds of volts) across the sheath [1,2,20]. The larger voltage drop can be attained partially by making the chuck holding the substrate to be small and also to be the ground rather than the driven electrode. Its smaller size (as compared to the driven electrode, which is made up of most of the rest of the chamber) results in a larger average ion current density and thus a higher average voltage drop through the sheath adjacent to the substrate. Higher input power also results in a greater voltage across the sheath.

At the pressures and sheath voltages used for ion-enhanced etching, the ions are accelerated through the sheath to higher energies (compared to chemical-plasma etching), which is transferred upon collision to the region being etched. The major component of the ion velocity is vertical, so ions tend to strike horizontal surfaces without touching the vertical sidewalls (Fig. 3). This is one of two factors leading to anisotropy in ion-enhanced plasma etching.

The ions can help drive a reaction (known as ion-enhanced energy-driven etching), or can aid in the removal of polymer films that have developed on horizontal surfaces (known as ion-enhanced inhibitor etching) [22]. (Polymer films are formed from carbon and fluorine or chlorine during the etch. The carbon can be supplied by the etch gas, the photoresist mask, or by a graphite electrode, while the halogen derives from the feed gases.) Polymer films that have formed on sidewalls remain to block chemical etching by neutrals (Fig. 3). The requirement of ions for the etch to occur is the second factor favoring anisotropic plasma etching.

The mean-free paths of the neutrals, like those of the ions, are longer at lower pressures. If the mean-free path is larger than the chamber dimensions, flow is effectively collisionless rather than diffusive.

Ion-enhanced etching is frequently referred to as "reactive-ion etching" (RIE), which is a misnomer [20]. The ions supply energy to some process in the etch, greatly increasing the etch rate beyond what a purely chemical etch would achieve. The ion flux is orders of magnitude too small to be responsible for the etching that does occur [1,22]. Radiation damage (e.g., lattice point defects), however, can result from the energetic ions in ion-enhanced etching [21]. The charging and damage of thin dielectric films (e.g., MOSFET gate oxides) by ions is another

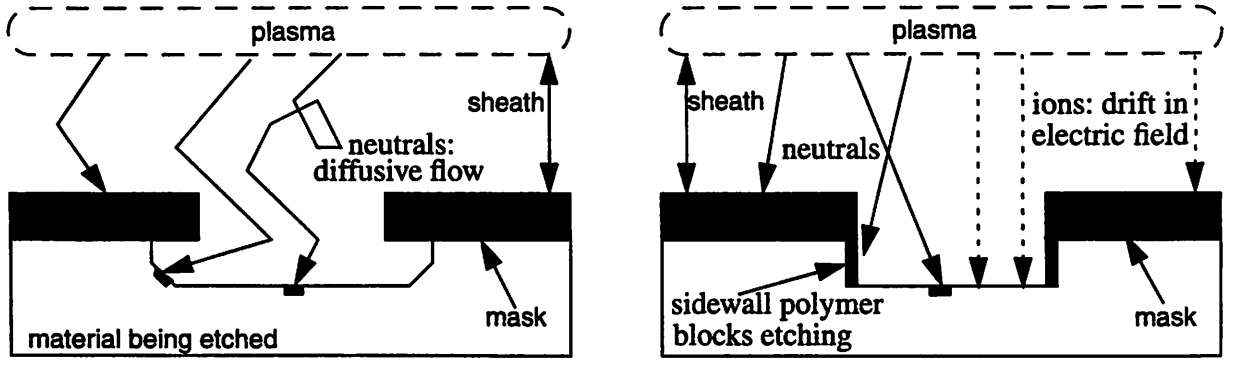

(a) Chemical-plasma etching:
all etching is done by neutrals.
Etching is isotropic.

(b) Ion-enhanced etching:
etching requires both neutrals and ions.
Etching is more vertical.

Figure 3 Chemical-plasma versus ion-enhanced-plasma etching.

concern in IC processing [23].

Sputter etching (also known as ion milling) is performed at lower pressures (in the 10-mTorr range), enabling ions to be accelerated through the sheath with few or no collisions. An inert gas (frequently argon) and an external dc bias are normally used. The energetic ions collide with substrate atoms, causing them to be ejected. Sputtering is purely physical (no chemical reaction occurs), so it is not as selective as chemical-plasma etching.

B. *Plasma-Etch Processes*

In plasma etching, there are gross similarities to the actions described earlier for wet etches (Fig. 2): (*a*) reactive species (radicals and ions) are generated in the bulk plasma; (*b*) these species are transported to the etch site by processes that may include forced flow (from the incoming gases), diffusion, or drift (of ions in an electric field) to a surface, followed by adsorption and diffusion along the surface; (*c*) a chemical or physical reaction takes place, which may require several sub-steps; and (*d*) the etch products leave the site, which may require diffusion along a surface, desorption, and diffusion back into the gas flow. The slowest of these steps is rate-limiting and determines the etch rate of the target material at a particular point on the wafer. As with wet etching, if two steps are of the same order of magnitude, the overall etch rate is less than the slower of the two.

The following approximate relations govern the four above steps.

(*a*) (*i*) *Generation of radicals*: The density of radicals in an electropositive plasma is given roughly by

$$n_{rad} = A_{rad} P n_{gas}^{b} \tag{9}$$

where A_{rad} is a constant that depends on the gas, P is the input power, n_{rad} and n_{gas} are the concentrations of radicals and input gas molecules (per unit volume), and b is a constant that varies from about 0.5 to 0.7, depending on the gas [22].

(*a*) (*ii*) *Generation of ions*: The density of ions at the edge of the sheath n_{is} in an electropositive plasma is given approximately by

$$n_{is} = A_{ion} P \tag{10}$$

where A_{ion} is a constant that depends on the gas, electrode area, and weakly on the pressure, and P is the input power.

(*b*) (*i*) *Flux in diffusive flow*: In steady-state lossless diffusive flow, the flux Γ is given by

$$\Gamma = D\frac{n_{bulk} - n_{surf}}{\delta} \tag{11}$$

where n_{bulk} and n_{surf} are the concentrations of a species in the bulk plasma at the surface (in particles per unit volume), D is the diffusivity, and δ is the boundary-layer thickness. The diffusivities of gases vary with temperature and pressure as

$$D = D_0\left(\frac{T}{T_0}\right)^{m}\left(\frac{p_0}{p}\right) \tag{12}$$

where D_0 is the diffusivity at T_0 and p_0 (any reference temperature and pressure) and m varies from 1.5 to 2.0, depending on the gas [4,24].

(*b*) (*ii*) *Flux in collisionless flow*: In collisionless flow, the flux of a given neutral species is given by

$$\Gamma = \tfrac{1}{4} n_g \bar{v}_g = \frac{n_g}{4}\left(\frac{8kT_g}{\pi m_g}\right)^{1/2} \tag{13}$$

where n_g is the gas density (in particles per unit volume), $\bar{v}_g$ is the average gas-molecule velocity in a given direction, T_g is the temperature of the gas molecules, and m_g is their mass [22]. The gas temperature depends primarily on the feed gas and chamber temperature, as discussed in a later section.

(*b*) (*iii*) *Adsorption, desorption, and surface diffusion*: Adsorption and diffusion rates on the surface are described by Arrhenius-factor equations. Likewise, the converse of the adsorption rate, the desorption rate DR, is given by

$$DR = A_{dr} T^{1/2} e^{-E_{dr}/kT} n'_{vm} \tag{14}$$

where A_{dr} is a constant, E_{dr} is the desorption activation energy, and n'_{vm} is the surface density of volatile molecules (in particles per unit area) [22].

(*c*) (*i*) *Reaction rate at the surface involving neutrals*: The reaction rate RR involving neutrals at the surface is typically given by an equation of the form

$$RR = K_0 e^{-E_{As}/kT_s} n'_g \tag{15}$$

where K_0 is a rate-constant prefactor, E_{As} is the reaction activation energy, T_s is surface temperature, and n'_g is the density of gas atoms covering the surface (in particles per unit area).

Most chemical-plasma etches are limited by the reaction rate at the surface [22]. An example is F-atom etching of Si. In this case, the surface gas density is proportional to the fluorine flux, which is proportional to $T^{1/2}$. Thus, the overall etch rate as a function of temperature is proportional to $T^{1/2} e^{-E_{As}/kT_s}$ [20].

(*c*) (*ii*) *Reaction rate at the surface involving ions*: In ion-enhanced etching, the ions aid in removal of a film. The equations are the same whether the film is an etch product or a polymer which blocks chemical etching. The etch rate involving ions at the surface is crudely given by

$$ER = K_i Y_i n_{is} n'_{film} = K_i \eta \frac{E_i}{E_b} A_{ion} P n'_{film} \tag{16}$$

where K_i is the rate constant for the ion-enhanced process, Y_i is the sputter yield (number of film molecules removed per incident ion), η is the sputtering efficiency, E_i is the ion energy, E_b is the binding energy of molecules in the film, n_{is} is the number of ions at the edge of the sheath (Eq. 10), A_{ion} is a constant, P is the input power, and n'_{film} is the density of film molecules adsorbed on the surface (in particles per unit area) [22].

(*d*) *Flux in diffusive flow, collisionless flow*, and *adsorption, desorption, and surface diffusion (after the surface reactions)*: A discussion of these processes follows that given previously as (*b*) (*i*) to (*iii*) above, with species leaving rather than moving toward the etch site.

As a practical matter, the predictive value of the relations discussed in this section is low. This is partially because they are approximate and partially due to interaction effects. As a practical matter, it is best to perform tests for an individual etching system to establish its performance under varying conditions.

C. *Plasma-Etch-Rate Variation*

Assuming that an etch chemistry (reactive gases and additives), reactor configuration (grounded or driven wafer holder), and RF-power supply (which sets the frequency and power range) have been selected, we have identified a number of factors that can affect plasma-etch rates. These sources of etch-rate variation can be divided into three categories: the etch setup, the material being etched, and the layout and structure on the substrate. The most significant

effects on plasma-etch rate in each category are as follows.

Etch-rate variation due to the etch setup is a function of (*i*) power, (*ii*) pressure, (*iii*) gas-flow rates, (*iv*) temperature, (*v*) film blocking of chemical flow, (*vi*) elapsed time from the start of the etch, (*vii*) materials present in the plasma chamber, (*viii*) changes in the etch chamber, and (*ix*) contamination. Etch-rate variation due to the material being etched is affected by (*x*) impurities in or on the material being etched, (*xi*) microstructure, and (*xiii*) film stress. Etch rates also vary as a consequence of the layout and structure due to the (*xii*) distribution and fraction of surface area of the target layer exposed, and (*xiv*) specimen structure geometry.

The manner in which the etch rate varies with each of these variables (some of which can be controlled, as summarized in Table 2) is discussed below. There are undoubtedly other factors that affect etch rates.

In addition to the target material, the etch rate of the masking layer will vary. These may vary at different rates, resulting in variation of selectivity.

(*i*) *Power*: If the etch rate is limited by the supply of reactants in the bulk plasma, it increases with power (Eq. 9). The etch rate also increases if the etch is diffusion-limited because the gradient from plasma to wafer surface rises (Eq. 11).

The sheath voltage is roughly proportional to the square root of the power, so higher power increases ion-bombardment energy. Near the threshold of ion-enhanced etching, increasing the power results in a large increase in etch rate as an inhibitor film is removed or ions supply energy to the etch [22]. Further increases in power continue to enhance the etch rate as long as the supply of ion energy is rate-limiting (Eq. 16).

(*ii*) *Pressure*: The chamber pressure is set by the pumping speed, the gas-flow rates, the power (higher power results in more dissociation of multiatomic feed gases), and the types of gases involved (some dissociate more readily than others). We assume for the following discussion that the pressure magnitude has been established for chemical-plasma or ion-enhanced etching, as discussed previously.

Changes in gas pressure under typical ion-enhanced etching conditions have a negligible effect on the plasma density (which is set primarily by the input power) [20]. The density of radicals in the bulk plasma, however, increases with pressure (Eq. 9).

Reactions involving gases, both in the bulk plasma and at surfaces, vary with pressure depending on the reaction order. The reaction rate depends on the product of the concentrations of each particle taking part in a reaction (cf. Eqs. 4 and 5), and therefore depends on the partial pressure of each (for atoms and molecules). Since the partial pressure for each gas is proportional to the total pressure, the reaction rates are proportional to some power of the pressure. First-order reactions, involving single gas molecules and a surface, vary linearly with pressure. Second-order reactions, involving two gas molecules, vary with the square of the total pressure. Third-order reactions, which involve three gas molecules in a rapid series of reactions (three-particle reactions are highly unlikely), vary with the cube of the pressure. Thus, if the formation of reactants in the plasma (second- or third-order) or surface reaction (first-order) is the rate-limiting step in an etch, the etch can be sped up by raising the pressure (assuming the ratio of individual gas partial pressures is unchanged).

Both diffusive (Eq. 12) and forced-flow motion of individual particles (as opposed to the overall flux as in Eq. 13) increase with decreasing total pressure. If the etch rate is limited by flow of reactants to the surface rather than by their production, lowering the total pressure may actually increase the etch rate by increasing the concentration at the surface. For diffusive-flow-limited etching, the etch rate may rise or fall, depending on the relative effects on diffusivity (Eq. 12) and the concentration gradient for the diffusing species (Eq. 11). Local

Plasma-Etch-Rate Variation				
User-Controlled Parameter	Limiting Step in the Etch	Pertinent Equation(s)	Approximate Effect	Explanation/ Assumptions
Power	Generation of reactants	$n_{rad}=A_{rad}Pn_{gas}^{0.6}$ $\Gamma=\frac{1}{4}n_{rad}\bar{v}_{rad}$	$ER\propto P$	Assumes reactants are used immediately.
	Diffusion of neutrals	$\Gamma=-D(n_{bulk}-n_{surf})/\delta$	$ER\uparrow$	n_{bulk} rises
	Reaction rate at surface involving neutrals	$RR=K_0e^{-E_A/kT}n_g'$ $n_{rad}=A_{rad}Pn_{gas}^{0.6}$	$ER\propto P$	Assumes the areal conc. n_g' is $\propto n_{rad}$.
	Polymer inhibitor removal or energy from ion flux	$ER=K_i\eta\frac{E_i}{E_b}A_{ion}Pn_{film}'$	$ER\uparrow$ faster than $\propto P$	Both ion flux and energy E_i rise with P.
Pressure	Generation of reactants	$RR=K_2n_1n_2e^{-E_A/kT}$ $\Gamma=\frac{1}{4}n_{rad}\bar{v}_{rad}$	$ER\propto p^n$	Assumes reactants are used immediately and gas fractions are constant.
	Diffusion through a boundary layer	$n_{bulk}\propto p^n$ $D=D_0\left(\frac{p_0}{p}\right)$ $\Gamma=-D(n_{bulk}-n_{surf})/\delta$	$ER\propto p^{n-1}$	ER assumes $n_{surf}\ll n_{bulk}$.
	Collisionless flux to surface	$n_{rad}=A_{rad}Pn_{gas}^{0.6}$ $\Gamma=\frac{1}{4}n_{rad}\bar{v}_{rad}$	$ER\propto p^{0.6}$	Assume reactants are used immediately.
	Reaction rate at surface	$n_{rad}=A_{rad}Pn_{gas}^{0.6}$ $SR=K_se^{-E_A/kT}n'$	$ER\propto p$	Assumes a first-order reaction.
	Polymer inhibitor removal or energy from ion flux	$ER=K_i\eta\frac{E_i}{E_b}A_{ion}Pn_{film}'$	$ER\downarrow$	Ion energy falls while ion density is about the same.
Flow Rate	Generation of reactants	$n_{rad}=A_{rad}Pn_{gas}^{0.6}$	$ER\uparrow$	Increased supply of reactants n_{gas}. Same pump speed.
	Loss of reactants to exhaust	-	$ER\propto 1/(flow\ rate)$	At very high flow rates, reactants are swept away.
Substrate Temperature	Generation of reactants (at low p)	$RR=K_1n_1e^{-E_{A1}/kT}$ $RR=K_2n_1n_2e^{-E_{A2}/kT}$	$ER\propto e^{-E_{A1}/kT}$	The substrate heats the gas.
	Generation of reactants (at high p)	-	0	The gas is at a different T than the substrate.
	Polymer inhibitor removal or energy from ion flux	-	0	Ion flux and energy are not affected by substrate temperature.
	Diffusion of neutrals through a boundary layer	$D=D_0\left(\frac{T}{T_0}\right)^{1.75}$	$ER\propto T^{1.75}$	Assumes main effect of T is on diffusivity.
	Collisionless flow of reactants	$\frac{n_g}{4}\left(\frac{8kT_g}{\pi m_g}\right)^{1/2}$	$ER\propto T^{1/2}$	Substrate heats the gas.
	Diffusion along a surface	$D=D_0e^{-E_M/kT}$	$ER\propto e^{-E_M/kT}$	Assumes a species must always surface diffuse.
	Desorption of Product Film	$DR=A_{dr}T^{1/2}e^{-E_d/kT}n_{vm}'$	$ER\propto T^{1/2}e^{-E_d/kT}$	Assumes the slowest step is desorption of a product film.

Table 2 User-Controllable Parameters in Plasma-Etch-Rate Variation

depletion of reactants occurs less at lower pressures, giving better uniformity in mass-transport-limited etching [20].

(*iii*) *Gas-flow rates*: For a given pumping speed, input gas-flow rates help to determine the pressure, causing the pressure effects discussed above.

The flow rate of a gas sets the etch rate if the supply of reactive atoms in the bulk plasma derived from that gas is the rate-limiting factor. In such cases, raising the flow rate raises the etch rate.

Raising the flow rate also enhances the etch rate of diffusion-limited etches by thinning the boundary-layer thickness δ (Eq. 11). Under laminar-flow conditions, δ is proportional to $1/\sqrt{v}$, where v is the free-flow gas velocity outside the boundary layer.

As in wet etching, the supply of reactants in dry etching can be depleted, and is most likely to occur in etches with a long residence time (i.e., low gas flow and low pumping speed). Depletion can cause uniform or localized etch-rate slowing, depending on the diffusion rate to the surface and the reaction rate there (e.g., a high surface-reaction rate and low diffusion rate can cause local etch-rate variation; a higher diffusion rate tends to equalize the etch rates across a surface). In plasma etching, one can increase the supply of fresh gaseous reactants by raising the flow rate and the pumping speed.

In the case of extremely high flow rates and pumping speeds, the residence time of reactive particles can be so short that many do not have a chance to reach the surface after being created before being swept from the chamber. In this limit, the etch rate is inversely proportional to the flow rate [20].

Finally, the gas-flow rates determine the the ratio of partial pressures of the gases in the chamber. Etch rates can vary greatly with the gas-flow ratio, depending on the series of reactions involved in the plasma.

(*iv*) *Temperature*: Temperature affects the rate of any surface or gas-phase reaction, typically as described by an Arrhenius equation, possibly with a temperature-dependent prefactor [20].

In plasma etching, one must distinguish between the surface, gas, and electron temperatures, as the system is not in thermal equilibrium. Due to the large mass ratio between electrons and other species, very little energy is passed from the energetic electrons during elastic collisions. Thus, the electrons remain "hot" (with energies of several eV), while the temperatures of the ions and gas atoms in the bulk plasma are determined by the feed-gas temperature and possibly by the chamber-wall temperature (with energies of a few hundredths of an eV). The reaction rates in the gas are governed by the temperatures of the gas particles involved.

The gas temperature within the thermal-boundary layer near the walls (which is much thicker than a mean-free path [3]), is close to the wall temperature [20]. Elsewhere in the chamber it is close to the temperature of the feed gas. Thus, at sufficiently low pressures, the gas-phase reaction rate can be enhanced by heating the chamber.

Surface-reaction rates can be increased or slowed by heating or cooling the surface. Selectivity can be improved by altering the temperature, taking advantage of activation-energy differences to speed up a desired reaction more than an undesired one. (For example, the activation energy for the etching of Si and SiO_2 in F are 0.107 and 0.163 eV, respectively, which favors Si etching at lower temperatures [20].) The overall etch rate places a practical limit on the maximum or minimum temperatures chosen.

In addition to affecting the reaction rate itself, temperature also affects the flux of reactants to the surface and thus the surface coverage. These can be modeled in an equation for the overall effect of temperature on the etch rate. An example is collisionless-flow F-atom etching

of Si. In this case, the surface coverage n_g' is proportional to the flux, which is proportional to $T^{1/2}$ (Eq. 13). Thus, the overall etch rate as a function of temperature is proportional to $T^{1/2}e^{-E_A/kT_s}$ (Eq. 15) [20]. The flux of reactants in diffusional flow is also enhanced at higher temperatures (Eq. 12).

In high-power-density etches, the wafer can be heated enough to affect various reactions, enhancing the etch rate during the course of an etch and for etches of subsequent wafers. In some cases, photoresist is eroded more easily. Such effects can be reduced by cooling the wafer and chamber, or by adding a wait step to the etch recipe.

In addition to changing the surface reaction rate, increasing the surface temperature decreases adsorption of reactants and increases desorption or evaporation of etch products (Eq. 14). Thus, a surface-temperature increase can slow etching that is limited by surface adsorption (e.g., plasmaless etching of Si in XeF_2 [20]), and speed etching that is limited by desorption of the etch products (e.g., the etch product of Al in Cl_2, Al_2Cl_6, is not very volatile at room temperature).

Temperature can also change the etch product. At room temperature, the product of F etching of Si is SiF_4. At higher temperatures, some SiF_2, which is normally an intermediate product, is able to leave as an unstable gas [20]. This does not affect the etch rate if the rate-limiting step has already occurred; otherwise, it increases the etch rate as later steps are bypassed.

(*v*) *Film blocking of chemical flow*: Films blocking chemical flow to impede an etch can include native oxides, etch products, and polymer films.

Native-oxide layers form on silicon and most metals. These can stop the etch if they are not removed by one of the species in the plasma (e.g., Al_2O_3 stops pure Cl_2 etching of Al). Functional plasma etches either already have a gas that results in removal of the native oxide (chemically or through ion bombardment), or have one added specifically for this purpose. Fluorine radicals, present in many plasma etches, remove most native oxides of interest.

If the etch products do not leave the surface, they can impede etching. For example, Al cannot be etched in an F-atom plasma because the product, AlF_3, is not volatile at normal processing temperatures. Al_2Cl_6 is more volatile, but heating of the surface is required for a reasonable desorption rate of this product.

Etch-blocking polymer films form on surfaces in the appropriate plasma chemistry. As they are typically removed with the aid of energetic ions in ion-enhanced etching, lower-flux or lower-energy ions result in slower etching if film removal is the rate-limiting step. Both can result from reduced input power.

Polymer-film formation is sensitive to feed-gas chemistry. For example, it has been found that for ratios of F atoms to C atoms in the plasma lower than about 3, polymer films stop the etching of Si and SiO_2 [1,25]. Increasing the ion-bombardment energy from zero to a few-hundred volts decreases the F-to-C ratio that causes etching to stop to about 2.2.

(*vi*) *Elapsed time from the start of the etch*: It normally takes several seconds for a plasma to stablize, so the etch rate will be different (typically lower) before steady-state operation has been established. Conversely, in plasmaless-gas-phase etching, the initial reactant supply may be higher than that in steady state. HF vapor, on the other hand, has been observed to require an incubation time for the formation of an HF/H_2O layer on the surface [26a].

(*vii*) *Materials present in the plasma chamber*: Materials other than the target layer present in the plasma chamber affect some plasma etch rates. These materials can be usefully divided into etchant consumers and polymer-film precursors (chamber contaminants are discussed separately in the following section).

Etchant consumers remove active species. They can include the target film, masking layer, and the layer under a target film. If etching at a point on the wafer is limited by the supply or flow of active species, the presence of a nearby consumer layer can slow the etch rate at that point. Thus, faster (but possibly less-uniform) etching may be achieved by changing from a masking film that is etched (e.g., photoresist in F) to one that is does not etch (e.g., Al in F).

The polymer-film precursors of carbon and fluorine (or carbon and chlorine in some cases [22]) are required for the formation of polymer films. The fluorine or chlorine is generally supplied by the feed gases, while the carbon can come from the feed gases, from an organic film, or from a graphite electrode. If the carbon source is an organic masking film on the wafer, changing to an inorganic or alternative organic mask may alter the supply of carbon. If less carbon is available for the formation of a film, a vertical ion-enhanced etch may become isotropic. If the film can grow at a faster rate on horizontal surfaces, the ion-enhanced etch rate on the horizontal surfaces decreases if it is controlled by the ion flux to the wafer.

(*viii*) *Changes in the Etch Chamber*: Changes in the etch chamber are primarily related to "wear" of the top electrode to which the driving voltage is applied (Fig. 2). This can change the electrode-wafer spacing, and, due to roughness, the electrode surface area. The result can be an altered and nonuniform etch rate.

(*ix*) *Contamination*: Because there are many possible types of contamination, it is difficult to predict all the effects contamination might contribute. The effects can be either an increased or a decreased etch rate of the target film. There can also be altered etch rates of the masking or underlying layers, which yields a change in selectivity (etch-rate ratio).

If a chamber is used for more than one process, it is possible that materials deposited on its walls during one etch can participate in the chemistry of subsequent etches.

Gases such as water vapor, if allowed to enter the chamber, can affect the etch rate. One effect of water vapor in plasmas is the generation of hydrogen ions (protons). These positive ions are much lighter and more mobile than their counterparts from other gases and are therefore able to carry a significant amount of the RF current. For a given input power, this decreases the current carried by the feed-gas cations, resulting in different ion densities and sheath voltages. This can result in increased etch rates. Since water vapor is present in room air, water molecules adsorb on the walls of an exposed vacuum chamber. Time is required for them to to desorb under vacuum, affecting the etch rate during that period. For example, the silicon plasma etcher in the Berkeley Microlab has an anodized aluminum electrode. The anodization is porous and the electrode can therefore absorb a lot of water vapor when exposed to the atmosphere (it is normally protected by an airlock). The water vapor desorbs slowly, resulting in greatly enhanced etched rates (up to 50%) for several days after exposure, depending on usage [26b].

(*x*) *Impurities in or on the material being etched*: As is the case for wet etching, impurities in the material being etched can affect the plasma-etch rate. For example, in F-atom plasmas, p-type silicon etches slightly more slowly than undoped silicon, while n^+ silicon etches faster [20]. In Cl-atom plasmas, however, n^+ silicon can be etched up to an order of magnitude more rapidly [20], although an effect this large has not been observed in the Berkeley Microlab (presumably because different etching systems were used). At Berkeley, phosphorus doping of LTO has been found to enhance the etch rate for all of the plasma chemistries tested for Table 4, while the etch rate of silicon-rich silicon nitride was always suppressed.

Films unintentionally covering the target layer can slow or stop the etch. Examples are undeveloped photoresist on any material and aluminum oxide on aluminum.

(*xi*) *Microstructure*: Microstructure affects the etch rate, both globally and locally, for the reasons discussed in the wet-etch-rate section: porous, defective, and small-grained films tend to

etch faster. Ion bombardment during plasma etching may introduce defects in a material, enhancing the rates of subsequent etching steps.

(*xii*) *Film Stress*: While the effect of film stress on plasma etching has received little study, it might be expected that, as with wet etching, the etch rate of a material will be affected by its stress state. Tensile films may etch slightly faster, as energy has been supplied mechanically, which reduces the energy required to remove atoms.

(*xiii*) *Distribution and fraction of surface area of the target layer exposed*: As is the case for wet etching, the distribution and fraction of surface area exposed in a plasma etch can affect both the overall and the local etch rates. Such loading effects, in which the etch decreases as the area being etched increases, are due to depletion of reactants at the surface (Eq. 15). For this reason, the plasma-etch rates for the 100%-exposure-area wafers in Table 4 may be considered as lower limits. The etch rate is uniformly lower if the etchant supply remains uniform with position. Frequently, however, the etch rate is fastest at the edge of the wafer (or at the edge of the wafer holder, for multi-wafer systems), as has been the experience in the Berkeley Microlab with the majority of the parallel-plate plasma etchers. This faster etching occurs when there is no etchant demand just outside the wafer periphery, resulting in a higher reactant concentration at the wafer edge. Nonuniform gas flow can result in oddly shaped etching patterns across a wafer. This has been observed in the XeF_2 etching of silicon.

In a mass-transport-limited etch, if the demand for reactants is not uniform across a wafer (because the masking layer is attacked more slowly than the target layer), etching varies with layout. Small, isolated openings etch more uniformly and rapidly than do large, closely spaced ones, in a miniature version of the effect described above for a whole wafer.

Etch-chemical demand changes near the end of an etch, as the target film disappears and underlying layers with different etch rates are exposed. The etch rate of the target film rises if the consumption by the newly exposed layer is lower, but falls if the demand rises.

Loading effects are common in plasma etching, and are one of the main concerns of equipment manufacturers. One of the solutions to the problem is the use of single-wafer processing, which decreases the area over which uniformity must be maintained. The use of "showerhead" gas ports in the top electrode greatly improves gas-distribution uniformity across the wafer.

(*xiv*) *Specimen structure geometry*: As with wet etching, high-aspect-ratio trenches and structures requiring significant undercutting are etched more slowly in the horizontal direction (aperture effect) for both chemical-plasma and ion-enhanced-plasma etching. For sufficiently long transport paths, etches are limited by diffusion of reactants to or of products from the etch site (Eq. 11).

IV. THE WET ETCHES

A. *Comparison of Wet and Plasma Etches*

The etches in the tables are divided into wet and plasma and plasmaless-gas-phase ("dry") etches. Wet etching was used for early generations of integrated circuits, but has been superseded for most IC processes by plasma etching. Wet etching is commonly used in micromachining, particularly for the orientation-dependent etching of silicon and for the removal of oxide sacrificial layers.

The advantages and disadvantages of wet and dry etching are well known [1,2]; the most important are as follows. Wet etching uses simpler, cheaper equipment, is usually isotropic

(desirable in some cases), and can be very selective. Plasma etching uses fresh chemicals for each etch, does not yield large quantities of chemicals requiring disposal, and can be anisotropic (as well as isotropic), allowing the patterning of narrow lines. However, plasma etching requires expensive systems of power supplies, reaction chambers, and vacuum pumps. When removing a sacrificial layer in micromachining, wet etching has the disadvantage of capillary-force pull-down of free-standing structures [27]. This can be avoided by using a supercritical-liquid drying process [28] or by switching to a plasma- or plasmaless-gas-etched sacrificial layer [29,30].

B. *Wet-Etch Chemicals*

All etching was done at room temperature (about 20°C in the temperature-controlled Berkeley Microfabrication Laboratory), unless otherwise indicated. All wet etching was done with fresh solutions, agitating occasionally.

Each etchant is listed by its name from Table 3 in italics, followed by its complete name, target material, notes on use, information on the reaction(s) that occur, if known, and major sources of etch-rate variations. For brevity, etchants with the same reactions are discussed together. The etchants are grouped by target material. Unless otherwise noted, all of the wet etchants are isotropic.

All mixtures done in the Berkeley Microlab, with a few noted exceptions, are by volume, while those made by chemical supply companies are by weight.

Acetic acid is supplied pure and sulfuric acid nearly pure (96%), while other acids normally come in lower concentrations for various reasons: Phosphoric acid is a deliquescent solid at room temperature [31]. Above the 85% concentration at which it is supplied, it is very viscous and tends to oligomerize into polyphosphoric acids. Pure hydrofluoric acid has a boiling point of 19.5°C [31]. As supplied at 49% concentration, it has a greatly reduced vapor pressure, increasing personal safety and allowing room-temperature storage in unpressurized containers. Nitric acid is a liquid in the range near room temperature, but tends to decompose above the supplied concentration of 70%. Sulfuric [32] and acetic [33] acids are liquids that are completely miscible in water at room temperature at all concentrations to 100%. Hydrofluoric acid [34] is also a completely soluble liquid below its boiling point.

An extensive list of other wet etchants for a variety of semiconductors, metals, insulators, and other compounds has been compiled by Vossen and Kern [7].

C. *Information about Individual Wet Etches*

1. *Silicon Dioxide Wet Etchants*

Notes: All of the silicon dioxide etchants given here are based on hydrofluoric acid. HF-based etchants are used mainly for etching silicon dioxide, although they can also be used to remove silicon nitride. In our tests, they were observed to etch polysilicon very slowly, but other researchers have noted that various solutions attack polysilicon at the grain boundaries, resulting in noticeable surface roughness [35,36]. Recent research indicates that HF can diffuse *through* thin (< 0.2-μm) polysilicon to etch underlying LTO [36,37].

HF-based solutions should be handled with polypropylene, high-density polyethylene (HDPE), polytetrafluoroethylene (PTFE), polyvinylidene fluoride (PVDF), or similar-material containers and tools (not glass containers, which will be attacked). In the Berkeley Microlab, molded PVDF has replaced welded polypropylene in most room-temperature chemical tanks in an effort to reduce particle counts and contamination from chemicals that have leaked into cracks in the welds. PTFE cassettes are used. All HF and other wet etching is done under fume

hoods to remove the vapors created by the etchants. Rubber gloves, face shields, and aprons are worn for personal protection.

Reaction: Several similar reactions for the HF-based etching of silicon dioxide are given in the literature. For pure HF etching, the overall reaction is [2,17]

$$SiO_2 + 6HF \rightarrow H_2SiF_{6(aq)} + 2H_2O \quad .$$

Kikuyama et al. give the reaction in BHF solutions as

$$SiO_2 + 4\,HF + 2\,NH_4F \rightarrow (NH_4)_2SiF_6 + 2\,H_2O$$

and the reaction involving the HF_2^- ion as [38]

$$SiO_2 + 3\,HF_2^- + H^+ \rightarrow SiF_6^{2-} + 2\,H_2O \quad .$$

HF is a weak acid; except when present in very small concentrations, it does not completely dissociate into H^+ and F^- ions in water. Judge [39] and Deckert [40] have found the etch rate of both silicon dioxide and silicon nitride to increase linearly with the concentrations of both HF and HF_2^- for concentrations lower than 10 M, while being independent of the concentration of F^- ions alone. The HF_2^- complex attacks oxide about 4.5 times faster than HF. Higher-order complexes, such as $H_2F_3^-$, appear to occur at higher HF concentrations (e.g., in 49% HF), and attack oxide even faster than HF_2^- [39]. Thus, the etch rate increases faster than linearly with HF concentration.

In buffered 15 M HF solutions, for pH values above about 1, the concentration of HF_2^- is greater than that of HF [39]. For more acidic solutions, there is sufficient hydrogen to combine with the fluoride to make HF the dominant species. As HF and HF_2^- are consumed, the etch rate decreases. Buffering with NH_4F helps keep the pH and thus the concentrations of HF and HF_2^- constant, stabilizing the etch rate.

The etch rate of silicon dioxide increases with temperature. Judge gives an apparent activation energy of 0.29 eV over the temperature range 30 to 60°C for concentrated HF, and higher activation energies as the ratio of NH_4F to HF increases [39]. By contrast, Parisi et al. found the apparent activation energy to be independent of buffer ratio at 0.43 eV over the range 25 to 55°C [41].

Tenny and Ghezzo found the etch rates of annealed phosphorus-doped LTO to increase monotonically with both P_2O_5 content and concentration of HF in BHF solutions [42], the same result found by Monk for HF solutions [36]. Tenny and Ghezzo concluded that the P_2O_5 in the glass is etched more rapidly than the SiO_2. They also found that for annealed borosilicate glasses, the etch rate in strong solutions of HF decreases for small concentrations of B_2O_3, before rising for concentrations above 17 molar percent.

Monk [36] has done a thorough characterization on the transport of HF and H_2SiF_6 during the undercutting of oxide sacrificial layers. He found that, for deep micromachined undercuts, the etch rate is controlled by diffusion (i.e., slower for longer undercutting), and is not affected by agitation of the bath.

Concentrated HF (49%): Concentrated hydrofluoric acid (49% by weight in water). Produced commercially.

Notes: Etches oxides very rapidly. Often used to remove sacrificial oxide when micromachining. Concentrated HF tends to peel off photoresist, while lower concentrations (less than 3:1) do not [43].

10:1 HF: 10:1 H_2O : concentrated HF (49% HF).

Notes: Typically used for stripping oxide and for HF dips, diluted HF is cheaper than buffered HF.

25:1 HF: 25:1 H_2O : concentrated HF (49% HF).

Notes: This slow etch is used for HF dips to strip native oxide without removing much of the other oxides on the wafer.

5:1 BHF: 5:1 buffered hydrofluoric acid (also known as buffered oxide etch, or BOE). "5:1" refers to 5 parts by weight of 40-weight-percent ammonium fluoride (the buffer) to 1 part by weight 49-weight-percent hydrofluoric acid, which results in a total of about 33% NH_4F and 8.3% HF, by weight [44]. Produced commercially. The *p*H is about 3.

Notes: This etch can be masked with photoresist (the adhesion is much better than in concentrated HF). Because it is buffered, its etch rate does not vary as much with use. It is the often best choice for controlled etching of oxides. Some researchers have, however, observed a slight attack of 5:1 BHF on polysilicon, causing surface roughening [35].

2. *Silicon Nitride Wet Etchant*

Phosphoric Acid (85%): Phosphoric acid (85% by weight, remainder H_2O) at 160°C. Produced commercially. In the Berkeley Microlab, this etchant is heated in a PFA tank with a Pyrex reflux system to return condensed water vapor to the solution.

Notes: Phosphoric acid is used for wet etching of silicon nitride. Our nitride is typically masked with densified PSG (densifying at 1000°C for an hour does not affect low-stress nitride). If the PSG mask is not densified it is removed faster and may also have pores through which the acid can seep. The nitride can also be masked with polysilicon.

At 160°C, the vapor pressure over 85% phosphoric acid is slightly more than one atmosphere, with the vapor being virtually pure water [45].

Reaction: The literature does not list a chemical reaction for the etching of silicon nitride. Gelder and Hauser propose that the water in the solution hydrolizes the nitride to some form of hydrous silica and ammonia [45].

Gelder and Hauser [45] report the "real" activation energy for the etching of silicon nitride in a constant concentration of 94.5% phosphoric acid as 0.99 eV. The "apparent" activation energies, taken with the etch temperature and boiling point being the same (i.e., for varying concentrations of H_3PO_4) are 0.55 eV for silicon nitride, 1.20 eV for silicon dioxide, and 1.15 eV for silicon. These apparent activation energies take into account the effects of temperature on both concentration of H_3PO_4 in the solution and the etch reactions themselves.

As the water content in the etch bath decreases (e.g., due to evaporation, the etch rate of silicon nitride decreases, while the etch rate of silicon dioxide increases [45], so the use of a reflux system is important in maintaining a constant etch rate and mask selectivity.

3. *Isotropic Silicon Wet Etchant*

Silicon Etchant: Wet silicon etchant. This solution is mixed and bottled in the Berkeley Microlab from 126:60:5 HNO_3 (70%) : H_2O : NH_4F (40%).

Notes: This etch, similar to the HNO_3 + H_2O + HF etches discussed in a series of papers by Robbins and Schwartz [2,46], is used mainly for polysilicon wet etching. The slight change in chemistry, used at Trilogy, provides some buffering for the HF concentration [47]. It can be masked by photoresist.

Reaction: A simplified description of the reaction is that the nitric acid in the solution oxidizes the silicon, then the hydrofluoric acid (formed from the fluoride ions in this acidic solution) etches the oxidized compound. Many metal etches not discussed in this paper remove material in this two-step manner. The overall reaction is [2,48]

$$18\ HF + 4\ HNO_3 + 3\ Si \rightarrow 3\ H_2SiF_{6\,(aq)} + 4\ NO_{(g)} + 8\ H_2O \quad .$$

Turner has found the peak etch rate of silicon to occur at an $HF:HNO_3$ ratio of 4.5, the same ratio as in the balanced reaction given above [48]. The rate-limiting step for the etch solution in this table, which has a low HF concentration, is the supply of HF to the reaction site [48]. The etch rate of a given bath decreases with use as the HF is depleted. The use of NH_4F rather than HF results in a buffer action, keeping the HF and HF_2^- (both responsible for etching the oxidized silicon) concentrations from changing as rapidly with use. Used solutions turn yellow due to dissolved NO gas.

4. *Orientation-Dependent Silicon Wet Etchants*

KOH 80°C: Potassium hydroxide solution at 80°C. Mixed from 1 kg KOH pellets : 2 liters H_2O. This solution is about 29% KOH by weight because the KOH pellets normally contain 10 to 15% water [49]. It is heated in a perfluoroalkoxy polytetrafluoroethylene (PFA) tank with recirculating pump.

Notes: This solution is self heating. It should be allowed to equilibrate before using for a controlled temperature. When etching single-crystal silicon (SCS), the silicon can be masked with silicon nitride. To reduce undercutting of the nitride mask, An HF dip should be carried out immediately before the nitride deposition to remove any native oxide.

We have found that the KOH in unagitated solutions tends to stratify, resulting in etch-rate variation from the top to the bottom of the solution. This problem was solved by the use of a recirculation pump.

KOH is used for orientation-dependent etching (ODE) of single-crystal silicon. ODEs attack {111}-type planes, which have a high bond density, much more slowly that other planes [2,50]. (Unfortunately, this high-bond-density reasoning for slow-etch-rate planes cannot be extended to explain the etch-rate ratio between {100} and {110} planes [50].) The etch rate listed in Table 3 is the one perpendicular to the surface of the (100) wafers used for this etch-rate test. KOH stops etching on very heavily doped *p*-type material [13].

Isopropyl alcohol is sometimes added to KOH solutions. This decreases the etch rate, but improves uniformity, reducing the requirement for stirring [5]. It also slows {110}-plane and accelerates {111}-plane etching (not affecting {100} planes much) and lessens the severity of the etching of convex corners [50].

(Other inorganic hydroxides [5,13], organic hydroxides such as Tetramethyl ammonium hydroxide (TMAH) [51,52], and ethylenediamine pyrocatechol (EDP) [5,13], an organic base, are orientation-dependent etchants similar to KOH. In the Berkeley Microlab and others, EDP has been found to be better than KOH at stopping abruptly at heavily boron-doped regions [13,14]. TMAH has the advantages of not being a source of sodium (which contaminates the gate oxide in MOS circuitry), and not attacking aluminum when it has been "doped" with a small amount of silicon [52].)

Reaction: Several different reactions for KOH etching of silicon are listed in the literature [2,5]. Seidel et al. list the gross reaction as [5]

$$Si + 2\ OH^- + 2\ H_2O \rightarrow SiO_2(OH)_2^{2-} + 2\ H_{2\,(g)} \quad .$$

Glembocki et al. list a very similar reaction [53] This chemical reaction is independent of the source of the hydroxide ion, whether LiOH, NaOH, or KOH, in agreement with experiment.

The dependence of the reaction on *p*-type doping is explained by Seidel et al. [5] and also by Raley et al. [14]: At intermediate steps in the etch, four free electrons are generated that reside near the surface before being exchanged. *P*-type doping reduces this surface supply of electrons. The etch rate decreases as the fourth power of the concentration for *p*-type doping beyond degeneracy, which occurs at about $2\times10^{19}cm^{-3}$ of active boron atoms.

Seidel found the etch-rate ratio for {110} to {100} to {111} planes to be about 160:100:1 at 20°C, decreasing to 50:30:1 at 100°C [5]. In contrast, Kendall measured even higher ratios of 400:200:1 at 85°C, and discussed the extreme difficulty in making these measurements [50].

The etch rate in KOH increases with temperature. Seidel et al. give activation energies for the concentration of KOH in Table 3 (33% by weight) of 0.61 eV for (100) silicon and 0.89 eV for silicon dioxide [5]. They also found that, at 80°C, the etch rates of (100) silicon and silicon dioxide peak at concentrations of about 18 and 34 weight %, respectively. Lower concentrations of either H_2O or OH^-, both used in the reaction, result in lower etch rates. The surfaces, however, appear rough and insoluble white residues form for KOH concentrations below 20% [54]. The temperature and KOH concentration effects on the etch rate (*ER*) of (100) silicon were empirically found to fit well to the equation [5]

$$ER_{Si\ in\ KOH} = k_0[H_2O]^4[KOH]^{1/4}e^{-E_A/kT}$$

where the etch rate is in μm/min, the concentrations are in mol/liter, k_0 = 2480 μm/hr·(mol/liter)$^{-4.25}$, and E_A = 0.595 eV.

5. *Metal Wet Etchants*

Aluminum Etchant Type A: Aluminum etchant Type A from bottle at 50°C. This solution, sold commercially, is composed of 80% phosphoric acid, 5% nitric acid, 5% acetic acid, and 10% water [55]. Some formulations may include a surfactant. According to the manufacturer, this etchant is designed to etch aluminum at 6000 Å/min at 50°C. It is heated in a PFA tank.

Notes: This etch is used for wet etching of aluminum. It can be masked with photoresist.

Reaction: In this multi-step etch [56], the aluminum is first oxidized by the nitric acid. The phosphoric acid and water simultaneously etch the resulting oxide. With the concentrations given, these two processes occur at roughly the same rate, so that either could be the rate-limiting step [56]. Because the phosphoric acid also removes the native aluminum oxide, no additional component is needed for this purpose.

The etch rate increases with temperature and decreases significantly with use due to depletion of the active chemicals.

Similar solutions with a reduced fraction of water etch more rapidly [56]. Agitating also increases the etch rate, as well as helping to remove the hydrogen bubbles that evolve. If not removed, these bubbles can block the flow of reactant to the surface, resulting in etch nonuniformity.

Titanium Etchant: Mixed from 20:1:1 H_2O : HF (49%) : H_2O_2 (30%).

Notes: HF is the active ingredient is this etchant, so it also etches oxides. Raising the fraction of HF in the solution increases the etch rate. Titanium etched in this solution can be masked with photoresist.

Reaction: No reaction is given in the literature. Titanium is known to be readily oxidized, so it likely forms an oxide from the water and peroxide, which is readily etched by the HF in this solution.

H_2O_2 (30%): Hydrogen peroxide (30% by weight). From bottle.

Notes: This etchant is used to wet-etch tungsten and its alloys, which can be masked with photoresist. We have observed that H_2O_2-etching of tungsten sometimes leaves a residue. We have also observed that when a titanium adhesion layer is used between tungsten and an underlying layer of phosphosilicate glass, and these films are annealed, that a thin conductive, optically transparent film is left after H_2O_2-etching of the tungsten. This film is not etched by a dilute HF solution, but can be removed in an SF_6 plasma.

Reaction: In this etch, a film of tungsten oxide is formed that is dissolved in the hydrogen peroxide [57]. This etchant also etches tungsten/titanium alloys, but not pure titanium.

The etch rate rises with temperature, but any significant increase may cause a photoresist mask to be eroded or to peel. CVD silicon-based masking layers, successful for other films, cannot be used with tungsten, as the silicon reacts to form tungsten silicides during the high-temperature deposition. Sputtered aluminum is a suitable mask layer, although when used, it becomes difficult to observe the end of the aluminum etch either optically or electrically.

(Another tungsten etch, which has been found in our lab not to leave the residue mentioned above, contains 1 liter H_2O, 34 g $K_3Fe(CN)_6$, 13.4 g KOH, and 33 g KH_2PO_4. It can be masked with photoresist, does not attack oxide or nitride at an appreciable rate, and etches tungsten at 340 Å/min.)

6. *Wet Wafer Cleaning*

Piranha 120°C: Piranha in 120°C heated bath. In the Berkeley Microlab, piranha consists of about 5.6 liters of 96% H_2SO_4 heated to 120°C in a PFA tank, to which 100 ml of 30% H_2O_2 is added immediately before use.

Notes: Piranha has been in use for wafer cleaning for decades [58,59]. This term refers is a hot solution of H_2SO_4 and H_2O_2 mixed in any ratio [58,59]. In lower ratios of H_2SO_4 to H_2O_2 (e.g., 5:1), the solution is noticeably self-heating (no external heat source is needed).

Piranha is used in the Berkeley Microlab for 10 minutes to clean organic and metallic contaminants from wafers before furnace steps. Kern and Puotinen [60] have observed that the desorption of 90% of monatomic metal films from silicon into similar acidic peroxide solutions can take several minutes.

Reaction: Like other acidic hydrogen peroxide solutions, piranha strips photoresist and other organics by oxidizing them, and removes metals by forming complexes that stay in the solution [60,61]. It does not affect silicon dioxide and silicon nitride, and has the minor effect on bare silicon of forming a thin layer of hydrous silicon oxide [60]. This oxide film is typically removed with a short (10- to 20-second) 10:1 or 25:1 HF dip after the piranha clean and rinse.

Acetone: Acetone spray from a photoresist developer.

Notes: Acetone is used to strip photoresist (PR) and for lift-off patterning of films [1]. The machine used in the Berkeley Microlab gives a stream of fresh acetone for PR stripping. An acetone bath would be used for liftoff processes. Liftoff processes can be sped up by heating the acetone (with a loose lid to slow evaporative loss) or by placing it in an ultrasonic tank.

While acetone readily stripped the photoresists listed in this table, its effectiveness depends on the processing the PR has gone through. Heating the PR by a few tens of degrees

above 120°C, either while hardbaking or during a process step, will make it significantly harder to dissolve [1]. Some plasma processing gives rise to a similar effect (known as "plasma hardening"). In such cases, an oxygen plasma, a commercial PR stripper (such as Baker PRS 2000), or piranha can usually be used to remove the PR.

Reaction: Acetone breaks down the structure of the photoresist, making it soluble [1].

V. THE PLASMA AND PLASMALESS-GAS-PHASE ETCHES

A. *Purposes of the Etch Gases*

Because many gases are used in more than one of the etches in Table 4, each gas (in italics) and its purpose are presented here.

Oxygen (O_2): O_2 dissociates into O radicals, which are more reactive. Oxygen has several purposes. Pure O_2 plasmas are used to etch photoresist. In plasmas involving CF_4, O atoms displace F in the CF_4 molecule, generating more free F [21]. This can both increase the etch rate and cause enough F to be present to allow the formation of C-F sidewall polymer films. O_2 is nontoxic at subatmospheric pressures [62] (long exposure to high-concentration O_2 burns lungs).

Sulfur Hexafluoride (SF_6): SF_6 is one source of very reactive F atoms, which etch all of the materials in Table 4 except for aluminum. Fluorine atoms are not very selective, etching most of these materials at rates varying by less than a factor of 5. Molecular fluorine (F_2) is not used for silicon etching because it is hazardous, and, for reasons not understood, it leaves rough surfaces [7,22]. SF_6 has a low order of toxicity [62,63].

Tetrafluoromethane (CF_4, carbon tetrafluoride, Freon 14): CF_4 is a source of F and also a source of C, both of which are required for C-F sidewall-polymer formation.

Trifluoromethane (CHF_3, Freon 23): CHF_3 is another source of F and C, but with a lower ratio of F to C. Like many fluorocarbons, CF_4 and CHF_3 are considered to be nontoxic [20,21].

Chlorine (Cl_2): Cl_2 dissociates into Cl atoms, which are quite reactive. Like F, Cl etches most materials, including aluminum. Cl_2 is toxic [64].

Trichloromethane ($CHCl_3$, chloroform): $CHCl_3$ supplies chlorine for etching and carbon and chlorine for sidewall polymer formation [22]. It is a mildly toxic [65,66].

Boron trichloride (BCl_3): BCl_3 etches the native aluminum oxide film on aluminum. It also scavenges O_2 and H_2O in the vacuum system, preventing oxide growth [20]. BCl_3 is a tissue irritant [67].

Helium (He): He can be used in plasma etching as a diluent and a plasma stabilizer [21]. Diluents give the user another process control variable. For example, an inert gas can be added to increase the total pressure while keeping the partial pressures of the other gases constant. In addition, some gas species can improve energy transfer from the "hot" electrons to reactive gas molecules (e.g., He enhances the dissociation of BCl_3 [21]). He, a noble gas, is nontoxic.

Nitrogen (N_2): N_2 is also used as a diluent. The main component of air, N_2 is nontoxic.

Hydrogen Fluoride Vapor (HF): HF vapor evaporates rapidly from concentrated HF solutions. Like its liquid counterpart, it is used for etching silicon dioxide. HF in contact with skin and mucous membranes causes severe burns.

Xenon difluoride (XeF_2): XeF_2 is supplied as granular crystals. At room temperature, it has an equilibrium vapor pressure of about 4.5 Torr [68]. XeF_2 supplies fluorine atoms in the plasmaless-gas-phase etching of silicon and some other materials. Supplying F atoms also makes XeF_2 a potent oxidizer [69]. Upon contact with water, hydrogen fluoride is formed, which burns the skin, eyes, and lungs [69].

Other gases: Many other gases in various combinations have been used for plasma etching, as discussed in several of the references [1,2,20-22].

B. *Information about Individual Plasma and Plasmaless-Gas-Phase Etches*

All of the plasma etches in Table 4 were done with recently cleaned chambers. The plasma and plasmaless-gas-phase etches are fairly isotropic unless otherwise noted. The plasma etches presented in this section have recipes that are based on the manufacturers' general recommendations for each machine, being adapted to yield a useful compromise among a reasonably fast etch rate for the target material, fairly straight sidewalls, selectivity over a photoresist mask layer, and (in most cases) uniformity across the wafer.

The etches are grouped by target material. The reactions listed are summaries; the occurrence of a complicated series of subreactions, adsorptions, and possibly energetic ion involvement should be considered typical. Details of some of the reactions are given in the references.

Each etch is listed by its name from Table 4 in italics, which includes the gases, their flow rates, equipment brand and model number, power, pressure, electrode gap, and operating frequency.

The plasmaless-gas-phase etchants, HF vapor and XeF_2, are listed with the plasma etches because they are more similar to chemical-plasma etching than to wet etching: reactant and product flow occurs in the gas phase and there is a fresh flow of reactants to the etch surface.

1. *Fluorocarbon-Plasma Silicon-Dioxide Etches*

Reaction: It appears that CF_x ($x \leq 3$) radicals chemisorb on the SiO_2 and dissociate. The radicals supply carbon to form CO, CO_2, and COF_2 gases from the oxygen in the film. They also supply fluorine to form SiF_4 gas [70]. Overall reactions such as the following occur [2]:

$$3\ SiO_2 + 4\ CF_3 \rightarrow 2\ CO + 2\ CO_2 + 3\ SiF_4$$

$$SiO_2 + 2\ CHF_2 \rightarrow 2\ CO + H_2 + SiF_4 \quad .$$

CF_4+CHF_3+He (90:30:130 sccm), Lam 590, 450W, 2.8T, gap=0.38cm, 13.56MHz: Parallel-plate configuration, graphite electrode (others are aluminum), driven electrode area ≈ 350 cm^2.

Notes: This etch targets silicon dioxide, but also etches silicon nitride well. It can be masked with photoresist. This etch is anisotropic (fairly vertical sidewalls).

If total etch times longer than about 2 minutes are required, the etch is often broken up into several shorter times, giving the PR a chance to cool and thus erode less.

CF_4+CHF_3+He (90:30:130 sccm), Lam 590, 850W, 2.8T, gap=0.38cm, 13.56MHz: Parallel-plate configuration, graphite electrode (others are aluminum), driven electrode area ≈ 350 cm^2.

Notes: This is a faster oxide etch than the lower-power etch above, but with lower selectivity to photoresist.

2. *Fluorine-Atom-Plasma Silicon-Nitride Etches*

Reaction: Fluorine atoms are adsorbed onto the surface one at a time. In a surface reaction, volatile products are formed. The overall reaction is [2]

$$Si_3N_4 + 12\ F \rightarrow 3\ SiF_4 + 2\ N_2 \quad .$$

The apparent activation energy for F-atom etching of Si_3N_4 is about 0.17 eV [20].

SF_6+He (13:21 sccm), Technics PE II-A, 100W, 250mT, 50kHz sq. wave: Parallel-plate configuration, fixed gap ≈ 2.6 cm, driven electrode area ≈ 600 cm^2 . The chamber holds four wafers; the test was performed with one wafer.

Notes: This etch is used to plasma-etch silicon nitride. It can be masked with photoresist.

This etch exhibits a severe loading effect. It is not only affected by the number of wafers in the chamber, but also by the fraction of nitride surface area that is exposed. Furthermore, the etch rate varies with position in the chamber, so wafers should be rotated 3-4 times during an etch (some users of this etcher also move their wafers among the four available wafer positions in a "planetary" motion).

Plasma etching, especially at higher power, heats the chamber, which can affect etch rates and thus selectivity. During all Technics PE II-A tests, the plate temperature varied from 20 to 30°C.

CF_4+CHF_3+He (10:5:10 sccm), Technics PE II-A, 200W, 250mT, 50kHz sq. wave : Parallel-plate configuration, fixed gap ≈ 2.6 cm, driven electrode area ≈ 600 cm^2 . The chamber holds four wafers; the test was performed with one wafer.

Notes: This silicon nitride plasma etch uses fluorocarbons rather than SF_6 as the source of F atoms.

SF_6+He (175:50 sccm), Lam 480, 150W, 375mT, gap=1.35cm, 13.56MHz: Parallel-plate configuration, driven electrode area ≈ 350 cm^2 .

This silicon nitride plasma etch is in a single-wafer system. The slower etch rate is intended for thin nitride films. It can be masked with photoresist. The etch is anisotropic (fairly vertical sidewalls).

SF_6+He (175:50 sccm), Lam 480, 250W, 375mT, gap=1.35cm, 13.56MHz: Parallel-plate configuration, driven electrode area ≈ 350 cm^2 .

Notes: This silicon nitride plasma etch is faster and therefore useful for thicker nitride films. It can be masked with photoresist. The etch is isotropic.

If total etch times longer than about 2 minutes are required, we break the etch up into several shorter times, giving the PR a chance to cool and thus erode less.

SF_6 (25 sccm), Tegal Inline Plasma 701, 125W, 200mT, 13.56MHz: Parallel-plate configuration, fixed gap ≈ 3.8 cm, driven electrode area ≈ 250 cm^2 .

Notes: This slower etch is intended for thinner, stoichiometric silicon nitride films.

CF_4+CHF_3+He (45:15:60 sccm), Tegal Inline Plasma 701, 100W, 300mT, 13.56MHz: Parallel-plate configuration, fixed gap ≈ 3.8 cm, driven electrode area ≈ 250 cm^2 .

Notes: This etch has a different gas chemistry than the previous etch, aimed at thicker, silicon-rich nitride films.

3. *Plasma Silicon Etches*

Cl_2+He (180:400 sccm), Lam Rainbow 4420, 275W, 425mT, 40°C, gap=0.80cm, 13.56MHz: Parallel-plate configuration, driven electrode area ≈ 390 cm^2 .

Notes: This is an anisotropic silicon plasma etch. An SF_6 step prior to this one is typically used to break through the native oxide.

This etch has been used to micromachine 80-μm-deep trenches with fairly vertical sidewalls [71].

Reaction: Chlorine atoms are chemisorbed one at a time on the silicon surface, eventually forming volatile $SiCl_4$ [20]. The overall reaction is

$$4\ Cl + Si \rightarrow SiCl_4 \quad .$$

Chlorine etching of undoped silicon occurs very slowly in the absence of ion bombardment [20]. Unlike F-atom silicon etches, Cl- and Br-based etches tend to be vertical [21].

As the Fermi level rises, the energy barrier for charge transfer of chemisorbed Cl, a step in the etch process, falls [20]. Thus, *p*-type doping slows etching while *n*-type doping accelerates it.

Chlorine-based plasma etch rates of single-crystal silicon can also depend on crystallographic orientation. Kinoshita and Jinno found that, with CCl_4+He plasmas, the {100} and {110} planes could be etched faster than the {111} planes [72]. The selectivity was not, however, as great as with KOH- or EDP-based etches.

$HBr+Cl_2$ (70:70 sccm), Lam Rainbow 4420, 200W, 300mT, 40°C, gap=0.80cm, 13.56MHz: Parallel-plate configuration, driven electrode area ≈ 390 cm^2.

Notes: This is another anisotropic silicon plasma etch, with better selectivity of silicon over oxide.

Reaction: Bromine atoms probably react with silicon in a manner similar to chlorine as described above.

4. *Plasma Metal Etches*

$Cl_2+BCl_3+CHCl_3+N_2$ (30:50:20:50 sccm), Lam 690, 250W, 250mT, 60°C, 13.56MHz: Parallel-plate grounded-chuck configuration, fixed gap ≈ 2.5 cm, driven electrode area ≈ 350 cm^2.

Notes: This is an anisotropic aluminum plasma etch due to the sidewall inhibitor formed from the $CHCl_3$ [22].

Due to poor selectivity, for thick layers of Al, thicker photoresist, plasma-hardened PR, or a more-durable masking layer must be used. The higher temperature is used to keep the etch product volatile so that it leaves the wafer [2] and does not coat the chamber or exhaust plumbing.

Reaction: The dominant overall reaction below 200°C [22] is

$$2\ Al + 3\ Cl_2 \rightarrow Al_2Cl_6 \quad .$$

Cl_2 rather than Cl appears to be the main etchant [22]. The etch product becomes $AlCl_3$ at higher temperatures [7,22].

All aluminum etches are followed by airlock plasma processing: CF_4=90 sccm, O_2 =10 sccm, P=400 W, for 1 minute. The airlock recipe is not intended to do any etching. It replaces the chlorine in the residual Al_2Cl_6 with fluorine. If this step were not performed, the chlorine would form hydrochloric acid upon exposure to atmospheric moisture, causing later corrosion of the aluminum.

SF_6 (80 sccm), Tegal Inline Plasma 701, 200W, 150mT, 40°C, 13.56MHz: Parallel-plate configuration, fixed gap ≈ 3.8 cm, driven electrode area ≈ 250 cm^2. Grounded chuck.

Notes: This tungsten plasma etch is fairly isotropic. CF_4 added to the feed gas increases anisotropy as sidewall polymers form, but slows the etch rate.

The chuck is heated to enhance the etch rate.

Reaction: The overall reaction is

$$W + 6\ F \rightarrow WF_6 \quad .$$

5. *Oxygen-Plasma Photoresist Etches*

Reaction: Oxygen atoms "burn" or "ash" the organic photoresist, forming mostly H_2O, CO_2, and CO [20]. Activation energies for O-atom etching of photoresist have been measured in the range of 0.22 to 0.65 eV [20]. Below 60°C, PMMA has an activation energy of about 0.2 eV [22].

O_2 (51 sccm), Technics PE II-A, 50W, 300mT, 50kHz sq. wave: Parallel-plate configuration, gap ≈ 2.6 cm, driven electrode area ≈ 600 cm^2. The chamber holds four wafers; the test was performed with one wafer.

Notes: This plasma-processing step is used for "descumming" (removing undesired thin layers) of freshly developed photoresist, typically for one minute. Unbaked OCG 820 PR was removed 6% faster than hardbaked PR during a descum test.

O_2 (51 sccm), Technics PE II-A, 400W, 300mT, 50kHz sq. wave: Parallel-plate configuration, fixed gap ≈ 2.6 cm, driven electrode area ≈ 600 cm^2 . The chamber holds four wafers; the test was performed with one wafer.

Notes: This oxygen plasma is used to ash (strip) photoresist for 5-10 minutes. A power of 300 W is also often used. It has been argued that lower power is better because there is less possibility of plasma hardening during stripping and of damage to MOS devices.

A loading effect, in which the etch rate decreases when there is more photoresist surface area, has been observed. In a 400 W PR stripping test, ashing four wafers at the same time was 23% slower than ashing one alone.

6. *Plasmless HF-Vapor Silicon-Dioxide Etch*

HF Vapor, 1 cm over plastic dish, Room temperature and pressure:

Notes: Like liquid-based HF etches, HF vapor etches silicon dioxide. It has been used to remove native oxide from silicon before the growth of epitaxial silicon [73] and other processes such as the XeF_2 etching of silicon.

In these tests, the HF/H_2O vapor condensed into droplets on the surfaces of the oxide samples during the one-minute etch, causing faster etching where these droplets had formed. This nonuniform etching can be greatly reduced by etching in "pulses," removing the wafer from the vapor before droplets form and allowing it to evaporate.

HF vapor may also be suitable for vapor-phase removal of a sacrificial oxide layer for micromechanical fabrication; however, caution should be used with photoresist masks, which peel (in these tests, the photoresist peeled when the wafers were rinsed).

In these tests, thermal oxide was etched at one third the rate of unannealed PSG. Other researchers have found that this selectivity goes up by two orders of magnitude when the wafers are heated to 50°C [26a].

Reaction: The overall reaction is [73]

$$SiO_2 + 4\ HF \rightarrow SiF_4 + H_2O \quad .$$

Water is assumed to catalyze the reaction [73], so a pure HF vapor may have a much slower etch rate than that over the 49% HF/51% H_2O used here. There is a brief incubation time at the beginning of the etch during which water molecules condense on the surface to be etched [73].

7. *Plasmaless XeF_2* Silicon Etch

XeF_2, Simple custom vacuum chamber, room temperature, 2.6 Torr:

Notes: XeF_2 was first synthesized in 1962 [74] and has been the subject of several papers on silicon etching [68,75], but was only recently "rediscovered" for its suitability for micromachining [76].

XeF_2 gas has the unusual capability to etch silicon at a significant rate without requiring a plasma to generate reactive species. As with chemical-plasma etching, etching is isotropic. The etched surface in deeply etched bulk silicon has been reported to have a roughness of several micrometers [76].

XeF_2 has been used to micromachine free-standing structures made of aluminum and polysilicon protected by a layer of oxide [76]. XeF_2 has the advantage over wet silicon etchants of gently etching without applying capillary forces, and the advantage over plasma etches of being extremely selective over almost all of the traditional masking layers, such as silicon dioxide, silicon nitride, and photoresist.

Because the native oxide on silicon surfaces completely stops etching, the silicon etch samples in these etch-rate tests were dipped in 10:1 HF, rinsed, and spun dry a few minutes before the etch rate tests. A period of 18 hours in a wafer box in room air was found sufficient to grow enough native oxide on doped polysilicon to stop etching completely.

The etching apparatus used for these etch-rate measurements consists of a source chamber containing XeF_2 crystals (with a 2.9-liter volume) separated by an inlet valve from the chamber where the etching takes place (with an 0.6-liter volume), which is connected to a roughing pump through an exhaust valve. The wafer is placed in the etch chamber, pumped down to its base pressure of about 12 mTorr, vented with dry nitrogen and pumped down again to reduce the amount of residual water vapor. Etching is initiated when the inlet valve is opened. Because of the large volume ratio of the source chamber to the etching chamber, the XeF_2 partial pressure remains about the same as its room-temperature equilibrium pressure after the valve is opened. Etching proceeds for 30 seconds before the inlet valve is closed. The exhaust valve is then opened for 30 seconds. For etches of total time longer than 30 seconds, this "pulsed-etching" cycle is repeated. All of the data reported here are for one minute of etch time.

The silicon etch rate in these tests varied greatly across the wafer, being higher in the stream beyond the gas inlet and slower to the sides. The etch rate of the single-crystal silicon wafer was higher in the areas adjacent to the photoresist mask. Attempting to reduce the etch-rate variation by increasing the pressure with dry nitrogen to about 100 mTorr resulted in one-tenth the original etch rate, but the same percentage uniformity (ratio of standard deviation of etch rate to average etch rate).

The etch rate has been reported to be extremely load-dependent [76], and measured values are as low as 11 nm/min when an entire 4-inch wafer is exposed to the XeF_2 to 10 μm/min for small chips of silicon.

It is possible that water vapor could result in the formation of HF, which then could attack oxide. An experiment to check this effect appeared to rule it out: When several drops

of water were placed on an oxide-covered wafer while in the etch chamber and allowed to vaporize into the chamber, the result was a higher base pressure before etching, but no etching of the oxide.

Adsorbed water has also been reported to result in the formation of a polymer-like film that inhibits etching [77]. Dehydration of silicon was recommended to avoid this problem.

To avoid possible problems resulting from adsorbed water vapor, the test wafers (except for the silicon samples) were dehydrated for several hours in flowing dry nitrogen at 120°C.

It has been found in our lab that as etch holes get deeper, the etch rate slows down. This may be due to a combination of local heating, which reduces the etch rate near room temperature [75], and the increasing area undergoing etching.

Reaction: XeF_2 molecules are physisorbed on the silicon surface [75] and dissociate to release volatile xenon atoms, while the fluorine atoms (not F_2 [68]) remain to react with the silicon to form volatile SiF_4. The overall reaction is

$$2\ XeF_2 + Si \rightarrow 2\ Xe + SiF_4 \quad .$$

The limiting step in the etching process appears to be the supply of fluorine atoms to the reaction site. Different steps in the supply processes dominate at different temperatures, causing a minimum in the etch rate of silicon as a function of temperature at around 410 K [75]. Ibotson et al. hypothesize that the etch rate increases below 410 K because the surface coverage of physisorbed XeF_2 is greater (the XeF_2 is less volatile), and this is the etch-rate-limiting step. When the etch-rate data at these lower temperatures were fitted to an Arrhenius equation of the form of Eq. 14 multiplied by the density of XeF_2, the effective activation energy was found to be negative at –0.14 eV (which corresponds to a positive activation energy for desorption). Above 410K the surface coverage is lower, but direct impact dissociation greatly increases the supply of fluorine atoms for the reaction. The effective activation energy for these higher temperatures was found to be 0.26 eV.

The etch rate of silicon has been observed to be proportional to the density of XeF_2 molecules for pressures below 0.5 Torr, rising less than linearly at higher pressures [75]. The etch rate has been found to be proportional to the incident flux of XeF_2 under flow that is force-blown perpendicular to the surface.

While according to several references, XeF_2 alone does not etch silicon dioxide and nitride (to the contrary, stoichiometric silicon nitride *was* etched slowly in our tests), it does etch these dielectrics in the presence of ion or electron bombardment and under UV radiation [68]. This may help to explain why fluorine atoms are nonselective in plasma etches.

VI. SAMPLE PREPARATION / MEMS APPLICATIONS

Most of the materials listed in the etch-rate tables are frequently used in the U. C. Berkeley Microfabrication Laboratory for micromachining and IC fabrication. The materials are identified in the following list, which shows the abbreviated material names from Tables 3 and 4 in italics. Preparation methods for the films are given, along with some MEMS applications and comments.

SC Si <100>: Single-crystal silicon, lightly doped with boron, with <100> orientation.

Single-crystal silicon is the standard starting material for bulk micromachining [78].

Poly n^+: In-situ heavily *n*-doped polycrystalline silicon. Refractive index (RI)=3.97.

Deposited on a wafer with thermal oxide already on it to enable interferometric thickness measurements. Deposited in a Tylan LPCVD furnace with the recipe SiH_4=120 sccm, PH_3=1 sccm, 605°C, p=300 mT. No anneal.

This deposition temperature and pressure were chosen to yield a low, tensile residual stress [15], which is suitable for micromachined beams and shells.

Poly, both doped and undoped, is a common MEMS structural material.

Poly undop: Undoped polycrystalline silicon. RI=3.97.

Deposited on a wafer with thermal oxide already on it to enable interferometric thickness measurements. Deposited in a Tylan LPCVD furnace with the recipe SiH_4=100 sccm, 605°C, p=300 mT. No anneal.

Wet Ox: Silicon dioxide thermally grown in water vapor. RI=1.46.

Grown in a Tylan atmospheric-pressure furnace with the recipe 1100°C, O_2 carrier gas at 200 sccm, H_2O vapor at a pressure just below 1 atm (the water source is at 98°C), and a total pressure of 1 atm, followed by a 20-minute N_2 anneal at 1100°C.

Thermal oxide has been used for thin sacrificial layers and for sealing cavities [79].

Dry Ox: Silicon dioxide thermally grown in dry oxygen. RI=1.46.

Grown in a Tylan atmospheric-pressure furnace with the recipe 1100°C, N_2=200 sccm, O_2=4000 sccm, p=1 atm, followed by a 30-minute N_2 anneal at 1100°C.

Dry oxidation, with its slow growth rate, can be used for very thin oxide layers of controlled thickness.

LTO undop: Undoped, annealed low-temperature oxide. RI=1.46.

Deposited in a Tylan LPCVD furnace with the recipe SiH_4=60 sccm, O_2=90 sccm, PH_3=0 sccm (no doping), 450°C, p=300 mT. Annealed in N_2 in a Tylan atmospheric-pressure furnace at 1000°C for 60 minutes.

LTO is used as a sacrificial layer, but it has a much slower etch rate than that of PSG in HF-based etches. It is only etched slightly faster than thermal oxides.

PSG unanl: Doped phosphosilicate glass with no anneal. RI=1.47.

Deposited in a Tylan LPCVD furnace with the recipe SiH_4=60 sccm, O_2=90 sccm, PH_3=10.3 sccm (considered a high doping level), T=450°C, p=300 mT.

Unannealed PSG has a much higher etch rate than annealed PSG. It has, however, been observed in the Berkeley Microlab to outgas during subsequent high-temperature steps, causing bubbling in overlying films, so it is not used as frequently as annealed PSG.

PSG annld: Doped, annealed phosphosilicate glass. RI=1.48.

Deposited in a Tylan LPCVD furnace under the same conditions as the unannealed PSG above, then annealed in N_2 in a Tylan atmospheric-pressure furnace at 1000°C for 60 minutes. This PSG has about 5.5 molar % P_2O_5 in SiO_2.

Oxides, usually chemical-vapor-deposited rather than thermally grown, are common sacrificial materials in micromachining. PSG (a doped LTO) etches much faster than undoped LTO in HF solutions, and is therefore preferred in structures requiring significant undercut.

Stoic Nitrid: Stoichiometric silicon nitride (Si_3N_4). RI=1.99.

Deposited in a Tylan LPCVD furnace with the recipe NH_3=75 sccm, SiH_2Cl_2=25 sccm, p=200 mT, T=800°C.

Stoichiometric silicon nitride is used in masking and for layers that are not free-standing.

High tensile residual stress precludes its use in free-standing structures.

Low-σ Nitrid: Low-stress silicon nitride (silicon-rich Si_xN_y). RI=2.18.

Deposited in a Tylan LPCVD furnace with the recipe NH_3=16 sccm, SiH_2Cl_2=64 sccm, p=300 mT, T=835°C.

Low-stress silicon nitride is used for optically transparent membranes and shells [80,81].

Al/2% Si: Sputtered aluminum with 2% silicon in the target.

Deposited in a CPA 9900 Sputtering System with the recipe p=4.5 kW, track speed=20 cm/min, p=6 mT. The substrate temperature was not controlled during sputtering and rose above room temperature.

Aluminum is used for interconnects and as a structural material in conjunction with organic sacrificial layers such as polyimide [29,30].

Sput Tung: Sputtered tungsten.

Deposited in a CPA 9900 Sputtering System with the recipe P=4.5 kW, track speed=10 cm/min, p=6 mT. The substrate temperature was not controlled during sputtering and rose above room temperature.

Tungsten, both sputtered (with thermal anneal for stress control) and CVD, is used for interconnects that can withstand high-temperature processing [82], as well as for a structural material [83].

Sput Ti: Sputtered titanium.

Deposited in a CPA 9900 Sputtering System with the recipe P=4.5 kW, track speed=10 cm/min, p=6 mT. The substrate temperature was not controlled during sputtering and rose above room temperature.

Titanium, being very reactive, is one of the few metals with good adhesion to oxide and nitride (aluminum and chromium are others). It is used as an adhesion layer for other, less-adhesive films, such as tungsten and gold.

Sput Ti/W: Sputtered 90% titanium/10% tungsten alloy.

Ti/W is used as an adhesion layer for sputtered and CVD tungsten.

OCG 820PR: OCG 820 (G-line sensitive) positive photoresist. RI=1.65.

Spun on using an SVG photoresist coater. Hardbaked 30 minutes at 120°C (experiments showed that baking for over 1 day had little difference on etch rate from 30 minutes of hardbaking).

For situations requiring a more durable resist, hardbaking at a higher temperature (up to 180°C), plasma hardening, or deep UV hardening can be done [1].

Photoresist hardening can also occur unintentionally during plasma etching. Difficult-to-remove PR can usually be removed in an oxygen plasma, piranha etch, or a commercial photoresist stripper (e.g., J. T. Baker PRS-2000 at 90°C).

In addition to masking, various photoresists [84] and other polymers [29,30] have been used as sacrificial layers in micromachining and as liftoff layers in patterning [1]. Photoresist has been etched with acetone, but oxygen plasmas are most common for micromachining removal of polymers, largely because no liquid is involved (liquid capillary forces cause free-standing structures to be pulled down as the liquid dries [27]).

Olin HntPR: Olin Hunt 6512 (I-line-sensitive) positive photoresist.

Spun on using an SVG photoresist coater. Hardbaked 30 minutes at 120°C. RI=1.63.

VII. ETCH-RATE MEASUREMENT TECHNIQUES

Transparent films (polysilicon, oxides, nitrides, photoresists) were each coated over an entire 100-mm (4-inch) wafer and etched without patterning. While 100% wafer area is rarely etched at once in MEMS and IC processing, a full-wafer etch was carried out to avoid effects caused by the presence of different materials in the etch. The film thicknesses were measured interferometrically with a NanoSpec AFT interferometric film-thickness-measurement system. Refractive indexes (RIs) were determined by ellipsometry and verified with the NanoSpec. These RIs are listed in the samples section of this report. (The apparent RI of the low-stress nitride films was significantly different when measured using the NanoSpec than by using the ellipsometer. We give the ellipsometer RI, which most often agrees with published data.)

Five locations on each wafer were measured before each etch, the films were etched, and then the same five locations (to within a few millimeters) were measured again. The average of the differences of these five points, divided by the etch time, determined the etch rate.

Opaque films (single-crystal silicon, metals) were etched several different ways to allow for measurement. Most of the metal etches were done with a photoresist masking layer. Previously patterned tungsten on a film of silicon nitride was used for tungsten in KOH and in the oxygen plasmas. Single-crystal silicon (SCS) with a nitride mask was used for SCS in KOH.

Five step heights distributed around the wafer were measured with a Tencor Alphastep 200 step profiler, the film was etched, then the same steps (to within a few tenths of a millimeter) were measured again. The average step-height difference (and the etch rate of the masking layer, if nonzero) were used to determine the etch rate of the film.

Wet etches having moderately fast rates (> 1000 Å/min) were done for one minute (even less for a few very rapid etches). Slower wet etches were done for at least 10 minutes to get a more accurate measurement. Samples with etch rates slower than 10 Å/min were etched for at least 30 minutes.

Plasma and plasmaless-gas-phase etching were done for one minute (or, for a few very rapid etches, for 30 seconds), with one wafer in the etch chamber. Care was taken to avoid plasma-hardening effects with the photoresist samples.

Accuracy of measurements: An etch rate is listed if the computed standard deviation was smaller than the average rate. In cases where the standard deviation was larger than the average (or the surfaces were very rough when Alphastep measurements were used), an upper limit equal to the average plus one standard deviation is given (e.g., < 50 Å/min). Etch rates of zero are recorded if the films were *thicker* after the etch, as often happened with photoresist (PR) in wet etches (the PR absorbed water). In a few cases, such as PR in acetone, the entire film was removed in a short time; a lower limit is listed for these etch rates (e.g. > 44kÅ/min). The measurements are rounded to two significant figures. The results are estimated to be accurate to within ±5% or ±5Å/min, whichever is smaller.

VIII. ETCH-RATE RESULTS

A. ETCH-RATE TABLES

Due to the amount of data, the etch-rate information is divided into two tables. Table 3 covers wet etches; Table 4 deals with plasma and plasmaless-gas-phase etches. (Tables covering all of the etches, in versions for outside and for Microlab use (with local equipment names), can be found at the end of the paper.) Etches are grouped by target material. Etch rates are reported in the commonly used units of angstroms per minute.

For each combination of material and etchant (e.g., n^+ poly and silicon etchant), the top value is the etch rate measured by the authors using fresh solutions, clean chambers, controlled temperatures, etc. (e.g., 3100 Å/min for n^+ poly in wet silicon etchant). The middle and bottom numbers are the slowest and fastest etch rates, respectively, observed by the authors or others in our laboratory during the past five years, using fresh and used solutions, "clean" and "dirty" plasma chambers, and looser temperature control (e.g., 1200 and 6000 Å/min for n^+ poly in silicon etchant). These observed variation ranges for etch rates are quite wide in a number of cases. Wider ranges usually occur for etches performed by many lab users. In some instances, the observed variation is small. This may either indicate that the etch is particularly repeatable or, perhaps, only a few results were reported by other lab users. An etch with a narrow range of reported rates should, therefore, not be construed as being particularly repeatable.

In some cases, an etch rate was not measured but something significant did happen. In cases in which the film (usually photoresist) peeled, a "P" denotes this. When the material was not etched significantly but was attacked forming a rough surface, an "A" denotes this.

Etch-rate tests for many of the combinations of materials and etches in the tables were not performed, often due to cross-contamination concerns in our lab's plasma-etching equipment. Where known, based on both published reports and local experience with the chemicals and materials involved, Tables 1 and 2 list whether 73 of the combinations will support an etch rate of at least 100 Å/min (denoted by a "W" in the tables), and whether the etch will be very fast (at least 10 kÅ/min, denoted by an "F").

Because etch rates vary due to many factors, *etch rates should not be expected to match those listed here exactly*. It is recommended that these etch rates be understood as order-of-magnitude correct and as valid when considering relative etch rates for different materials. Sources of etch-rate variation were discussed earlier in this paper.

B. DISCUSSION OF ETCH-RATE DATA

- Several conclusions can be drawn from the data in the etch-rate tables. Some are considered common knowledge among those familiar with semiconductor processing or are expected from the literature on the subject.
- Wet etches tend to be more selective than plasma etches. Plasma etches using SF_6, CF_4, or CHF_3, which supply fluorine radicals, are particularly nonselective.
- For hydrofluoric-acid-based etching of various types of silicon dioxide, we find that for weaker concentrations of HF (going from 25:1 to 10:1), the etch rate increases almost linearly with concentration, but rises much faster going to concentrated HF. No difference in the etch rates of wet and dry thermally grown silicon dioxide is observed.
- Annealing PSG greatly slows its etch rate in most wet etches, but does not affect the plasma-etch rate significantly. Annealed, undoped LTO etches much more slowly in all of the wet etches, and slightly more slowly in the plasma etches than the annealed PSG (doped LTO),

Wet-Etch Rates for Micromachining and IC Processing (Å/min)

The top etch rate was measured by the authors with fresh solutions, etc. The center and bottom values are the low and high etch rates observed by the authors and others in our lab under less carefully controlled conditions.

ETCHANT / EQUIPMENT / CONDITIONS	TARGET MATERIAL	MATERIAL															
		SC Si <100>	Poly n+	Poly undop	Wet Ox	Dry Ox	LTO undop	PSG unanl	PSG annld	Stoic Nitrid	Low-σ Nitrid	Al/ 2% Si	Sput Tung	Sput Ti	Sput Ti/W	OCG 820PR	Olin HntPR
Concentrated HF (49%) Wet Sink Room Temperature	Silicon oxides	-	0	-	23k 18k 23k	F	>14k	F	36k	140	52 30 52	42 0 42	<50	F	-	P 0	P 0
10:1 HF Wet Sink Room Temperature	Silicon oxides	-	7	0	230	230	340	15k	4700	11	3	2500 2500 12k	0	11k	<70	0	0
25:1 HF Wet Sink Room Temperature	Silicon oxides	-	0	0	97	95	150	W	1500	6	1	W	0	-	-	0	0
5:1 BHF Wet Sink Room Temperature	Silicon oxides	-	9	2	1000 900 1080	1000	1200	6800	4400 3500 4400	9	4 3 4	1400	<20 0.25 20	F	1000	0	0
Phosphoric Acid (85%) Heated Bath with Reflux 160°C	Silicon nitrides	-	7	-	0.7	0.8	<1	37	24 9 24	28 28 42	19 19 42	9800	-	-	-	550	390
Silicon Etchant (126 HNO_3 : 60 H_2O : 5 NH_4F) Wet Sink Room Temperature	Silicon	1500	3100 1200 6000	1000	87	W	110	4000	1700	2	3	4000	130	3000	-	0	0
KOH (1 KOH : 2 H_2O by weight) Heated Stirred Bath 80°C	<100> Silicon	14k	>10k	F	77 41 77	-	94	W	380	0	0	F	0	-	-	F	F
Aluminum Etchant Type A (16 H_3PO_4 : 1 HNO_3 : 1 HAc : 2 H_2O) Heated Bath 50°C	Alumnium	-	<10	<9	0	0	0	-	<10	0	2	6600 2600 6600	-	0	-	0	0
Titanium Etchant (20 H_2O : 1 H_2O_2 : 1 HF) Wet Sink Room Temperature	Titanium	-	12	-	120	W	W	W	2100	8	4	W	0 0 <10	8800	-	0	0
H_2O_2 (30%) Wet Sink Room Temperature	Tungsten	-	0	0	0	0	0	0	0	0	0	<20	190 190 1000	0	60 60 150	<2	0
Piranha (~50 H_2SO_4 : 1 H_2O_2) Heated Bath 120°C	Cleaning off metals and organics	-	0	0	0	0	0	-	0	0	0	1800	-	2400	-	F	F
Acetone Wet Sink Room Temperature	Photoresist	-	0	0	0	0	0	-	0	0	0	0	-	0	-	>44k	>39k

Notation: - =test not performed; W=not performed, but known to *W*ork (≥ 100 Å/min); F=not performed, but known to be *F*ast (≥ 10 kÅ/min); P=some of film *P*eeled during etch or when rinsed; A=film was visibly *A*ttacked and roughened.
Etch areas are all of a 4-inch wafer for the transparent films and half of the wafer for single-crystal silicon and the metals.
Etch rates will vary with temperature and prior use of solution, area of exposure of film, other materials present (e.g., photoresist), film impurities and microstructure, etc. *Some variation should be expected.*

Table 3 Wet-etch rates

Plasma- and Plasmaless-Gas-Phase-Etch Rates for Micromachining and IC Processing (Å/min)

The top etch rate was measured by the authors and others in our lab with clean chambers, etc. The center and bottom values are the low and high etch rates observed by the authors and others under less carefully controlled conditions.

ETCHANT / EQUIPMENT / CONDITIONS	TARGET MATERIAL	MATERIAL: SC Si <100>	Poly n+	Poly undop	Wet Ox	Dry Ox	LTO undop	PSG unanl	PSG annld	Stoic Nitrid	Low-σ Nitrid	Al/ 2% Si	Sput Tung	Sput Ti	Sput Ti/W	OCG 820PR	Olin HntPR
CF_4+CHF_3+He (90:30:120 sccm)	Silicon	W	1900	2100	4700	W	4500	7300	6200	1800	1900	-	W	W	W	2200	2000
Lam 590 Plasma	oxides		1400	1500	2400			3000	2500								
450W, 2.8T, gap=0.38cm, 13.56MHz			1900	2100	4800			7300	7200								
CF_4+CHF_3+He (90:30:120 sccm)	Silicon	W	2200	1700	6000	W	6400	7400	6700	4200	3800	-	W	W	W	2600	2900
Lam 590 Plasma	oxides		2200	1700	2500		6000	5500	5000	4000						2600	2900
850W, 2.8T, gap=0.38cm, 13.56MHz			2700	2100	7600		6400	7400	6700	6800						6700	7200
SF_6+He (13:21 sccm)	Silicon	300	730	670	310	350	370	610	480	820	620	-	W	W	W	690	630
Technics PE II-A Plasma	nitrides	300	730	670					230		550					690	
100W, 250mT, gap=2.6cm, 50kHz sq. wave		1000	800	760					480		800					830	
CF_4+CHF_3+He (10:5:10 sccm)	Silicon	1100	1900	W	730	710	730	W	900	1300	1100	-	W	W	W	690	600
Technics PE II-A Plasma	nitrides																
200W, 250mT, gap=2.6cm, 50kHz sq. wave																	
SF_6+He (175:50 sccm)	Thin	W	6400	7000	300	W	280	530	540	1300	870	-	W	W	W	1500	1400
Lam 480 Plasma	silicon			2000	220					830						1300	
150W, 375mT, gap=1.35cm, 13.56MHz	nitrides			7000	400					2300						1500	
SF_6+He (175:50 sccm)	Thick	W	8400	9200	800	W	770	1500	1200	2800	2100	-	W	W	W	3400	3100
Lam 480 Plasma	silicon									2100						3100	
250W, 375mT, gap=1.35cm, 13.56MHz	nitrides									4200						3400	
SF_6 (25 sccm)	Thin	W	1700	2800	1100	W	1100	1400	1400	2800	2300	-	W	W	W	3400	3100
Tegal Inline Plasma 701	silicon				1100					2800						2900	
125W, 200mT, 40°C	nitrides				1600					2800						3400	
CF_4+CHF_3+He (45:15:60 sccm)	Si-rich	W	350	360	320	W	320	530	450	760	600	-	W	W	W	400	360
Tegal Inline Plasma 701	silicon																
100W, 300mT, 13.56MHz	nitrides																
Cl_2+He (180:400 sccm)	Silicon	W	5700	3200	8	-	60	230	140	560	530	W	W	-	-	3000	2700
Lam Rainbow 4420 Plasma		5000	3400	3200	8											2400	
275W, 425mT, 40°C, gap=0.80cm, 13.56MHz		5000	6300	3700	380											3000	
HBr+Cl_2 (70:70 sccm)	Silicon	W	450	460	4	-	0	0	0	870	26	W	W	-	-	350	300
Lam Rainbow 4420 Plasma			450		4											350	
200W, 300mT, 40°C, gap=0.80cm, 13.56MHz			740		10											500	
Cl_2+BCl_3+$CHCl_3$+N_2 (30:50:20:50 sccm)	Aluminum	W	4500	W	680	670	750	W	740	930	860	6000	W	-	-	6300	6300
Lam 690 RIE												1900				3700	3300
250W, 250mT, 60°C, 13.56MHz												6400				6300	6100
SF_6 (80 sccm)	Tungsten	W	5800	5400	1200	W	1200	1800	1500	2600	2300	-	2800	W	W	2400	2400
Tegal Inline Plasma 701					2000						1900		2800			2400	
200W, 150mT, 40°C, 13.56MHz					2000						2300		4000			4000	
O_2 (51 sccm)	Descumming	-	0	0	0	0	0	0	0	0	0	0	0	0	-	350	300
Technics PE II-A Plasma	photoresist																
50W, 300mT, gap=2.6cm, 50kHz sq. wave																	
O_2 (51 sccm)	Ashing	-	0	0	0	0	0	0	0	0	0	0	0	0	-	3400	3600
Technics PE II-A Plasma	Photoresist																
400W, 300mT, gap=2.6cm, 50kHz sq. wave																	
HF Vapor	Silicon	-	0	0	660	W	780	2100	1500	10	19	A	0	A	-	P 0	P 0
1 cm over plastic dish	oxides																
Room temperature and pressure																	
XeF_2	Silicon	4600	1900	1800	0	-	0	0	0	120	2	0	800	290	-	0	0
Simple custom vacuum chamber		2900	1100	1100						120	0		440	50			
Room temperature, 2.6 Torr		100k	2500	2300						180	2		1000	380			

Notation: - =test not performed; W=not performed, but known to *W*ork (≥ 100 Å/min); F=not performed, but known to be *F*ast (≥ 10 kÅ/min); P=some of film *P*eeled during etch or when rinsed; A=film was visibly *A*ttacked and roughened.
Etch areas are all of a 4-inch wafer for the transparent films and half of the wafer for single-crystal silicon and the metals.
Etch rates will vary with temperature and prior use plasma chamber, area of exposure of film, other materials present (e.g., photoresist), film impurities and microstructure, etc. *Some variation should be expected.*

Table 4 Plasma- and plasmaless-gas-phase-etch rates

approaching the slow etch rate of the thermal oxides.

• N^+ polysilicon etches faster than undoped poly in the silicon wet etchant and in the chlorine-based plasma, but the two etch at roughly the same rate in the fluorine-based plasmas.

• Stoichiometric silicon nitride etches at the same rate or faster than the silicon-rich low-stress nitride in all of the etches except HF vapor.

• Tungsten is removed slowly or not at all in all of the wet etches, including HF and KOH solutions, making it a candidate for a structural material in micromachined devices.

• Titanium is etched so much faster than most oxides in HF solutions that it is possible to stop a titanium etch on oxide.

• The etch rates of the two types of positive photoresist studied are within 15% of each other in most of the etches, with neither photoresist always being etched more slowly or rapidly. In results not reported in the table, we varied the hardbake time of the OCG 820 from its standard 30 minutes to 1 hour and 1 day. Surprisingly, this had a negligible effect on the removal rate.

• The oxygen plasmas, intended for descumming and stripping photoresist, attack only photoresist.

• Piranha, intended for cleaning metals and organics from wafers, attacks only the metals and photoresists in these tests.

• Xenon difluoride selectively etches silicon, as well as titanium and tungsten. It unexpectedly (but repeatedly) also etches stoichiometric silicon nitride, but not silicon-rich nitride.

IX. END-OF-ETCH DETECTION

In some etches, it is easy to see when the film being etched has cleared to expose an underlying layer of another color. Sometimes this can be seen unaided; other times a microscope is necessary. In many situations, however, it is difficult to tell whether an etch is complete and more sophistication is needed. Following are some such situations (listed in italics) and comments about etch-end detection.

In all cases, due to the possibility of etch-rate nonuniformity, several locations on the wafer should be checked, particularly the center and the edges of the wafer. Steps in the underlying substrate may result in "stringers" remaining after vertical anisotropic etches, so these areas, too, should be checked.

Clear film on the substrate: Etch completeness can be tested by measuring the film thickness in a window in the mask using an interferometer or ellipsometer.

Conductive film on nonconductive layer: A conductive film can be tested by measuring the resistance by microprobing two adjacent points on the area being etched. A quantitative check of etch progress can be obtained by measuring the resistance at the same region on the wafer, with the same probe spacing, before and after etching. The etch is complete when an open circuit is detected with an ohmmeter or curve tracer. (We have found a curve tracer applying a few volts to be useful in breaking down a thin films of native oxide, polymer films, residue on the probe tip, or other nonconductive layers, which might register as an open circuit with an ohmmeter.) This technique is also useful for checking for "stringers" (narrow lines of residual film remaining at the bottoms of steps in topography). A "sanity check" can be done by scratching through the photoresist to check the resistance of the unetched film.

Nonconductive film on conductive layer: Etch completeness can be detected by microprobing two points on an area being opened up by the etch. The etch is complete when a short circuit is observed with a curve tracer or ohmmeter.

Any film with a mask layer that is etched slowly: If the film- and mask-layer thicknesses are known, a step profiler can be used to measure the step height.

ACKNOWLEDGMENTS

We thank Katalin Voros of the Berkeley Microfabrication Laboratory, Chris Keller and Michael Houston of the Berkeley Sensor & Actuator Center, Igor Kouzneteov of the Plasma Simulation and Theory Group, and Nathan Cheung of Electrical Engineering and Computer Sciences, all at the University of California at Berkeley, for reviewing this paper and providing constructive criticism. We also thank Robert Hamilton of the Berkeley Microlab for providing information about etching equipment. This work was supported by the Berkeley Sensor & Actuator Center.

REFERENCES

[1] S. Wolf and R. N. Tauber, *Silicon Processing for the VLSI Era, vol. 1.* Sunset Beach, Calif.: Lattice Press, 1986.

[2] W. R. Runyan and K. E. Bean, *Semiconductor Integrated Circuit Processing Technology.* Reading, Mass.: Addison-Wesley Pub. Co., 1990.

[3] Hermann Schlichting, *Boundary Layer Theory.* New York: McGraw-Hill Book Co., 1960, Ch. 2 and 14.

[4] W. Jost, *Diffusion in Solids, Liquids, Gases.* New York: Academic Press, Inc., 1952, Chs. 10 and 11.

[5] H. Seidel, L. Csepregi, A. Heuberger, and H. Baumgartel, "Anisotropic etching of crystalline silicon in alkaline solutions, I. Orientation dependence and behavior of passivation layers, " *J. Electrochem. Soc.*, vol. 137, no. 11, pp. 3612-3626, Nov. 1990.

[6] O. J. Glembocki, E. D. Palik, "Hydration model for the molarity dependence of the etch rate of Si in aqueous alkali hydroxides," *J. Electrochem. Soc.*, vol. 138, no.4, pp. 1055-63, April 1991.

[7] John L. Vossen and Werner Kern, eds., *Thin Film Processes.* New York: Academic Press, 1978, Chapter V-1.

[8] Rolfe Carter Anderson, "Formation, properties, and applications of porous silicon," Ph. D. dissertation in Chemical Engineering, University of California at Berkeley, 1991.

[9] A. Uhlir, Jr., "Electrolytic shaping of germanium and silicon," Bell System Tech. J., vol. 35, pp. 333-347, 1955.

[10] Henry Nielsen and David Hackleman, "Some illumination on the mechanism of SiO_2 etching in HF solutions," *J. Electrochem. Soc.*, vol. 130, no. 3, pp. 708-712, Mar. 1983.

[11] M. J. J. Theunissen, "Etch channel formation during anodic dissolution of N-type silicon in aqueous hydrofluoric acid," *J. Electrochem. Soc.*, vol. 119, no. 3, pp. 351-360, Mar. 1972.

[12] C. V. Macchioni, "The effect of substrate temperature and bias on the stress, chemical etch rate, and microstructure of high deposition rate sputtered SiO_2 films," *J. Vac. Sci. Technol. A*, vol. 9, no. 4, pp. 2302-2308, Jul./Aug. 1991.

[13] H. Seidel, L. Csepregi, A. Heuberger, and H. Baumgartel, "Anisotropic etching of crystalline silicon in alkaline solutions, II. Influence of dopants, " *J. Electrochem. Soc.*, vol. 137, no. 11, pp. 3626-3632, Nov. 1990.

[14] N. F. Raley, Y. Sugiyama, and T. Van Duzer, "(100) silicon etch-rate dependence on boron concentration in ethylenediamine-pyrocatechol-water solutions," *J. Electrochem. Soc.*, vol. 131, no. 1, pp. 161-171, Jan. 1984.

[15] P. Krulevitch, R. T. Howe, G. C. Johnson, and J. Huang, "Stress in undoped LPCVD polycrystalline silicon," *Tech. Dig. 6th Int. Conf. on Solid-State Sensors (Transducers '91)*, San Francisco, Calif., June 1991, pp. 949-952.

[16] Denny A. Jones, *Principles and Prevention of Corrosion.* New York: Macmillan Publishing Co., 1992, p. 290.

[17] Sorab K. Ghandi, *VLSI Fabrication Principles.* New York: John Wiley & Sons, 1983, Chapter 9.

[18] Ion Stiharu, Rama Bhat, Mojtaba Kahrizi, and Leslie Landsberger, "The influence of the stress state in silicon on the anisotropic etching process," *Proc. SPIE*, vol. 2015, (*Laser-Assisted Fabrication of Thin Films and Microstructures*), Quebec, Canada, pp. 254-262, Aug. 1993.

[19] E. A. Irene, D. W. Dong, and R. J. Zeto, "Residual stress, chemical etch rate, refractive index, and density measurements on SiO_2 films prepared using high pressure oxygen," *J. Electrochem. Soc.*, vol. 127, no. 2, pp. 396-399, Feb. 1980.

[20] Dennis M. Manos and Daniel L. Flamm, Eds., *Plasma Etching: An Introduction.* Boston: Academic Press, Inc., 1989.

[21] Stephen M. Rossnagel, Jerome J. Cuomo, and William D. Westwood, Eds., *Handbook of Plasma Processing Technology.* Park Ridge, New Jersey: Noyes Publications, 1990.

[22] Michael A. Lieberman and Allan J. Lichtenberg, *Principles of Plasma Discharges and Materials Processing.* New York: John Wiley & Sons, Inc., 1994.

[23] Hyungcheol Shin and Chenming Hu, "Monitoring plasma-process induced damage in thin oxide," *IEEE Transactions on Semiconductor Manufacturing*, vol. 6, no. 2, pp. 96-102, May 1993.

[24] Dwight E. Gray, Ed., *American Institute of Physics Handbook.* New York: McGraw-Hill Book Co., Inc., 1957, pp. 2-211 and 2-213.

[25] J. W. Coburn and H. F. Winters, "Plasma etching--a discussion of mechanisms," *J. Vac. Sci. Technol.*, vol. 16, no. 2, pp. 391-403, Mar.-Apr. 1979.

[26a] Man Wong, Mehrdad M. Moslehi, and Robert A. Bowling, "Wafer temperature dependence of the vapor-phase HF oxide etch," *J. Electrochem. Soc.*, vol. 140, no. 1, pp. 205-

208, Jan. 1993.

[26b] Alan Miller of Lam Research, personal communication, Oct. 3, 1995.

[27] C. H. Mastrangelo and C. H. Hsu, "Mechanical stability and adhesion of microstructures under capillary forces--Part II," *J. Microelectromech. Syst.*, vol. 2, no. 1, pp. 44-55, March 1993.

[28] Gregory T. Mulhern, David S. Soane, and Roger T. Howe, "Supercritical carbon dioxide drying of microstructures," *Tech. Dig. 7th Int. Conf. on Solid-State Sensors and Actuators (Transducers '93)*, Yokahama, Japan, June 1993, pp. 296-299.

[29] J. B. Sampsell, "The digital micromirror device and its application to projection displays," *Tech. Dig. 7th Int. Conf. on Solid-State Sensors and Actuators (Transducers '93)*, Yokahama, Japan, June 1993, pp. 24-27.

[30] C. W. Storment, D. A. Borkholder, V. Westerlind, J. W. Suh, N. I. Maluf, and G. T. A. Kovacs, "Flexible, dry-released process for aluminum electrostatic actuators," *J. Microelectromech. Syst.*, vol. 3, no. 3, pp. 90-96, Sept. 1994.

[31] Robert C. Weast, Ed., *CRC Handbook of Chemistry and Physics, 66th Ed.*. Boca Raton, Florida: CRC Press, Inc., 1985 pp. B-67 - B-161.

[32] George L. Clark, Ed., *The Encyclopedia of Chemistry, 2nd Ed.*. New York: Reinhold Publishing Co., 1966. [33] Gessner G. Hawley, *The Condensed Chemical Dictionary, 8th Ed.*. New York: Van Nostrand Reinhold Co., 1971.

[34] J. W. Mellor, *A Comprehensive Treatise on Inorganic and Theoretical Chemistry*. London: Longmans, Green and Co. Ltd., 1927, vol. 2.

[35] R. L. Alley, G. J. Cuan, R. T. Howe, and K. Komvopoulos, "The effect of release-etch processing on surface microstructure stiction," *Tech. Dig. IEEE Solid-State Sensor and Actuator Workshop*, Hilton Head, South Carolina, June 1992, pp. 202-207.

[36] David Joseph Monk, "Controlled structure release for silicon surface micromachining," Ph. D. dissertation in Chemical Engineering, University of California at Berkeley, 1993.

[37] Kyle S. Lebouitz, Roger T. Howe, and Albert P. Pisano, "Permeable polysilicon etch-access windows for microshell fabrication," *Tech. Dig. 8th Int. Conf. on Solid-State Sensors and Actuators (Transducers '95)*, Stockholm, Sweden, June 1995, pp. 224-227.

[38] Hirohisa Kikyuama, Nobuhiro Miki, Kiyonori Saka, Jun Takano, Ichiro Kawanabe, Masayuki Miyashita, Tadahiro Ohmi, "Principles of wet chemical processing in ULSI microfabrication," *IEEE Trans. Semicon. Manuf.*, vol. 4, no. 1, pp. 26-35, Feb. 1991.

[39] John S. Judge, "A study of the dissolution of SiO_2 in Acidic Fluoride Solutions," *J. Electrochem. Soc.*, vol. 118, no. 11, pp. 1772-1775, Nov. 1971.

[40] Cheryl A. Deckert, "Etching of CVD Si_3N_4 in Acid Fluoride Media," *J. Electrochem. Soc.*, vol. 125, no. 9, pp. 320-323, Feb. 1978.

[41] G. I. Parisi, S. E. Haszko, and G. A. Rozgonyi, "Tapered windows in SiO_2: the effect of NH_4F:HF dilution and etching temperature," *J. Electrochem. Soc.*, vol. 124, no. 6, pp. 917-921, Jun. 1977.

[42] A. S. Tenny and M. Ghezzo, "Etch rates of doped oxides in solutions of buffered HF," *J.*

Electrochem. Soc., vol. 120, no. 8, pp. 1091-1095, Aug. 1973.

[43] R. A. Haken, I. M. Baker, and J. D. E. Beynon, "An investigation into the dependence of the chemically-etched edge profiles of silicon dioxide on etchant concentration and temperature," *Thin Solid Films*, vol. 18, no. 1, pp. S3-S6, Oct. 1973.

[44] J. T. Baker, Inc., "Product Specifications for Product No. 5192, Buffered Oxide Etch, 5:1," J. T. Baker, Inc., Phillipsburg, New Jersey, 1993. technical support, June 7, 1995.

[45] W. van Gelder and V. E. Hauser, "The etching of silicon nitride in phosphoric acid with silicon dioxide as a mask," *J. Electrochem. Soc.*, vol. 114, no. 8, pp. 869-872, Aug. 1967.

[46] H. Robbins and B. Schwartz, "Chemical Etching of Silicon I," *J. Electrochem. Soc.*, vol. 106, pp. 505-508, 1961.

[47] Ping K. Ko, formerly of EECS at U. C. Berkeley, personal communication, June 11, 1996.

[48] D. R. Turner, "On the mechanism of chemically etching germanium and silicon," *J. Electrochem. Soc.*, vol. 107, no. 10, pp. 810-816, Oct. 1960.

[49] Fisher Chemical/Fisher Scientific, "Bottle label of potassium hydroxide, solid," Fisher Chemical, Fair Lawn, New Jersey, 1996.

[50] Don L. Kendall, "A new theory for the anisotropic etching of silicon and some underdeveloped chemical micromachining concepts," *J. Vac. Sci. Technolog. A*, vol. 8, no. 4, pp. 3598-3605, Jul./Aug. 1990.

[51] O. Tabata, R. Asahi, H. Funabashi, K. Shimoka, and S. Sugiyama, "Anisotropic etching of silicon in TMAH solutions," *Sensors and Actuators A*, vol. 34, no. 1, pp. 51-57, Jul. 1992.

[52] U. Schnakenberg, W. Benecke, and P. Lange, "TMAHW etchants for silicon micromachining," *Tech. Dig. 1991 Int. Conf. on Solid-State Sensors and Actuators (Transducers '91)*, San Francisco, 1989, pp. 815-818.

[53] O. J. Glembocki, E. D. Palik, G. R. de Guel, and D. L. Kendall, "Hydration model for the molarity dependence of the etch rate of Si in aqueous alkali hydroxides," *J. Electrochem. Soc.*, vol. 138, no. 4, pp. 1055-1063, Apr. 1991.

[54] H. Seidel, "The mechanism of anisotropic silicon etching and its relevance for micromachining," *Tech. Dig. 4th Int. Conf. on Solid-State Sensors and Actuators (Transducers '87)*, Japan, 1987, pp. 120-125. Also in R. S. Muller, et al., eds., *Microsensors*. New York: IEEE Press, 1991, pp. 104-109.

[55] Transene Co. Inc., "Material safety data sheet for aluminum etchant Type A," Transene Co., Inc., Rowley, Mass., 1987.

[56] David J. Elliot, *Integrated Circuit Fabrication Technology, 2nd Ed.*. New York: McGraw-Hill Publishing Co., 1989, p. 355.

[57] J. E. A. M. van den Meerakker, M. Scholten, and J. J. van Oekel, "The etching of Ti-W in concentrated H_2O_2 solutions," *Thin Solid Films*, vol. 208, no. 2, pp. 237-242, Feb. 1992.

[58] Michael G. Yang and K. M. Koliwad, "Auger electron spectroscopy of cleanup-related contamination on silicon surfaces," *J. Electrochem. Soc.*, vol. 122, no. 5, pp. 675-678, May 1975.

[59] F. Pintchovski, J. B. Price, P. J. Tobin, J. Peavey, and K. Kobold, "Thermal characteristics of the H_2SO_4–H_2O_2 silicon wafer cleaning solution," *J. Electrochem. Soc.*, vol. 126, no. 8, pp. 1428-1430, Aug. 1979.

[60] Werner Kern and David A. Puotinen, "Cleaning solutions based on hydrogen peroxide for use in silicon semiconductor technology," *RCA Review*, vol. 30, no. 2, pp. 187-206, Jun. 1970.

[61] J. A. Amick, "Cleanliness and the cleaning of silicon wafers," *Solid State Technology*, vol. 19, no. 11, pp. 47-52, Nov. 1976.

[62] William Braker and Allen L. Mossman, Eds., *Matheson Gas Data Book.* Secaucus, New Jersey: Matheson Gas Products, 1980.

[63] Matheson Gas Products, Material Safety Data Sheet for SF_6, Brisbane, Calif., Oct. 1985.

[64] Frank A. Patty, Ed. *Industrial Hygiene and Toxicology, 2nd Edition, Vol. II: Toxicology*, New York: Interscience Pub. Div., John Wiley & Sons, Inc., 1963.

[65] Matheson Gas Products, Material Safety Data Sheet for $CHCl_3$, Brisbane, Calif., Oct. 1985.

[66] Susan Budavari, Ed., *The Merck Index.* Rahway, N. J.: Merck & Co., Inc., 1989.

[67] Matheson Gas Products, Material Safety Data Sheet for BCl_3, Brisbane, Calif., Oct. 1985.

[68] H. F. Winters and J. W. Coburn, "The etching of silicon with XeF_2," *Applied Physics Letters*, vol. 34, no. 1, pp. 70-73, Jan. 1979.

[69] Johnson Matthey/Alfa Aesar, Material Safety Data Sheet for XeF_2, Ward Hill, Mass., Mar. 1995.

[70] S. M. Sze, Ed. *VLSI Technology.* New York: McGraw Hill Book Co., 1983, Chapters 2 and 8.

[71] Chris G. Keller and Roger T. Howe, "Nickel-filled hexsil thermally actuated tweezers," *Tech. Dig. 8th Int. Conf. on Solid-State Sensors and Actuators (Transducers '95)*, Stockholm, Sweden, June 1995, pp. 376-379.

[72] H. Kinoshita and K. Jinno, "Anisotropic etching of silicon by gas plasma," *Japanese J. Applied Physics*, vol. 16, no. 2, pp. 381-382, Feb. 1977. *J. Electrochem. Soc.*, vol. 131, no. 9, pp. 161-171, Jan. 1984.

[73] A. E. T. Kuiper and E. G. C. Lathouwers, "Room-temperature HF vapor-phase cleaning for low-pressure chemical vapor deposition of epitaxial Si and SiGe layers," *J. Electrochem. Soc.*, vol. 139, no. 9, pp. 2594-2599, Sep. 1992.

[74] David W. Oxtoby and Norman H. Nachtrieb, *Principles of Chemistry.* Philadelphia: Saunders College Publishing, 1986, p. 728.

[75] Dale E. Ibotson, Daniel L. Flamm, John A. Mucha, and Vincent M. Donnelly, "Comparison of XeF_2 and F-atom reactions with Si and SiO_2", *Applied Physics Letters*, vol. 44, no. 12, pp. 1129-1131, June 1984.

[76] E. Hoffman, B. Warneke, E. Kruglick, J. Weigold, K. S. J. Pister, "3D Structures with piezoresistive sensors in standard CMOS," *Proceedings of IEEE Micro Electro Mechanical Systems 1995*, Amsterdam, Netherlands, Jan.-Feb. 1995, pp. 288-293.

[77] Kristofer S. J. Pister of University of California, Los Angeles, personal communication, Mar. 24, 1995.

[78] K. E. Petersen, "Silicon as a mechanical material," *Proc. IEEE*, vol. 70, no. 5, pp. 420-457, May 1982. Also in R. S. Muller, et al., eds., *Microsensors*. New York: IEEE Press, 1991, pp. 39-76.

[79] H. Guckel and D. W. Burns, "Fabrication techniques for integrated sensor microstructures," *Tech. Dig. Int. Electron Devices Meeting 1986*, Los Angeles, 1986, pp. 176-179.

[80] M. Sekimoto, H. Yoshihara, and T. Ohkubo, "Silicon nitride single-layer x-ray mask," *J. Vac. Sci. Technol.*, vol. 21, no. 4, pp. 1017-1021, Nov./Dec. 1982.

[81] C. H. Mastrangelo and R. S Muller, "Vacuum-sealed silicon micromachined incandescent light source," *Tech. Dig. IEEE Int. Electron Devices Mtg.*, Dec. 1989, pp. 503-506.

[82] Clark T.-C. Nguyen and Roger T. Howe, "CMOS micromechanical resonator oscillator," *Tech. Dig. IEEE Int. Electron Devices Mtg.*, Dec. 1993, pp. 199-202.

[83] K. R. Williams and R. S. Muller, "IC-processed hot-filament vacuum microdevices," *Tech. Dig. IEEE Int. Electron Devices Mtg.*, Dec. 1992, pp. 387-390.

[84] Kent Erik Mattson, "Surface micromachined scanning mirrors," *Microelectronic Engineering*, vol. 19, pp. 199-204, 1992.

BIOGRAPHIES

Kirt R. Williams was born in Walnut Creek, California in 1964. He received the B.S. degree with high honors with a double major in Electrical Engineering and Computer Sciences (EECS) and Materials Science and Engineering from the University of California at Berkeley in 1987. While studying for this degree, he worked at the Eastman Kodak Company and Altera Corporation, and after graduation, went to Western Digital Corporation to do digital and analog circuit design. Mr. Williams has been performing graduate work with the Berkeley Sensor & Actuator Center at U.C. Berkeley since 1989, earning the M.S. degree in EECS in 1993. His main area of study is MEMS, with a thesis on micromachined hot-filament vacuum devices. Mr. Williams has also been active in teaching and updating the department's IC-fabrication laboratory class, for which he received the EECS Outstanding Graduate Student Instructor Award in 1996.

Richard S. Muller received the degree of Mechanical Engineer (with highest honor) from Stevens Institute of Technology and the MS/EE and Ph.D. at the California Institute of Technology. He joined the faculty in the Department of EECS at the University of California, Berkeley in 1962 and was promoted to full Professor in 1972. He is one of two founders, and presently a co-director of the Berkeley Sensor & Actuator Center, an NSF/Industry/University research center. He has been awarded NATO and Fulbright Research Fellowships at the Technical University, Munich, Germany; is an Alexander von Humboldt senior-scientist award winner; has been appointed a Guest Professor at the Swiss Federal Institute of Technology (Zurich); and has been awarded the U.C. Berkeley Citation (1994); and Stevens Institute of Technology Renaissance Award (1995). Professor Muller is a member of the National Academy of Engineering of the United States, a Fellow of the IEEE, an IEEE Distinguished Lecturer, the Chairman of the Sensors Advisory Board, and member of the Advisory Committee for the Electron-Devices Society of IEEE. He has been designated an IEEE/EDS Distinguished Lecturer for 1994/95. Professor Muller has served as chairman of the steering committee for the biennial Transducers Conference, the North American Technical Program Chairman of Transducers '89, and the General Chairman of Transducers '91. He serves on the IEEE Press Editorial Board and proposed, helped found, and is presently an Editor-at-large for the IEEE/ASME *Journal of Microelectromechanical Systems* (JMEMS). Dr. Muller is also the North American Editor of *Sensors & Materials*, and on the editorial boards of *Sensors and Actuators* and *Nanotechnology*. Together with Dr. T. I. Kamins of Hewlett-Packard Co., he is the author of *Device Electronics for Integrated Circuits*, (Wiley) second edition, 1986. He is a co-editor of *Microsensors*, a volume in the IEEE Press Selected Reprint Series, published in 1990. Professor Muller is the author or co-author of more than 200 technical papers and conference presentations and of fifteen issued patents.

Etch Rates for Micromachining and IC Processing (Å/min) v. 4.4 29 July 1996

U.C. Berkeley Microfabrication Laboratory / Berkeley Sensor & Actuator Center / Kirt R. Williams

The top etch rate was measured by the author with fresh solutions, clean chambers, etc.

The center and bottom values are the low and high etch rates observed by the author and others in the UCB Microlab using fresh and used solutions, clean and "dirty" chambers, etc.

ETCHANT / EQUIPMENT / CONDITIONS	TARGET MATERIAL	MATERIAL															
		SC Si <100>	Poly n+	Poly undop	Wet Ox	Dry Ox	LTO undop	PSG unanl	PSG annld	Stoic Nitrid	Low-σ Nitrid	Al/ 2% Si	Sput Tung	Sput Ti	Sput Ti/W	OCG 820PR	Olin HmtPR
Concentrated HF (49%) Wet Sink Room Temperature	Silicon oxides	-	0	-	23k 18k 23k	F	>14k	F	36k	140	52 30 52	42 0 42	<50	F	-	P 0	P 0
10:1 HF Wet Sink Room Temperature	Silicon oxides	-	7	0	230	230	340	15k	4700	11	3	2500 2500 12k	0	11k	<70	0	0
25:1 HF Wet Sink Room Temperature	Silicon oxides	-	0	0	97	95	150	W	1500	6	1	W	0	-	-	0	0
5:1 BHF Wet Sink Room Temperature	Silicon oxides	-	9	2	1000 900 1080	1000	1200	6800	4400 3500 4400	9	4 3 4	1400	<20 0.25 20	F	1000	0	0
Phosphoric Acid (85%) Heated Bath with Reflux 160°C	Silicon nitrides	-	7	-	0.7	0.8	<1	37	24 9 24	28 28 42	19 19 42	9800	-	-	-	550	390
Silicon Etchant (126 HNO_3 : 60 H_2O : 5 NH_4F) Wet Sink Room Temperature	Silicon	1500	3100 1200 6000	1000	87	W	110	4000	1700	2	3	4000	130	3000	-	0	0
KOH (1 KOH : 2 H_2O by weight) Heated Stirred Bath 80°C	<100> Silicon	14k	>10k	F	77 41 77	-	94	W	380	0	0	F	0	-	-	F	F
Aluminum Etchant Type A (16 H_3PO_4 : 1 HNO_3 : 1 HAc : 2 H_2O) Heated Bath 50°C	Alumnium	-	<10	<9	0	0	0	-	<10	0	2	6600 2600 6600	-	0	-	0	0
Titanium Etchant (20 H_2O : 1 H_2O_2 : 1 HF) Wet Sink Room Temperature	Titanium	-	12	-	120	W	W	W	2100	8	4	W	0 0 <10	8800	-	0	0
H_2O_2 (30%) Wet Sink Room Temperature	Tungsten	-	0	0	0	0	0	0	0	0	0	<20	190 190 1000	0	60 60 150	<2	0
Piranha (~50 H_2SO_4 : 1 H_2O_2) Heated Bath 120°C	Cleaning off metals and organics	-	0	0	0	0	0	-	0	0	0	1800	-	2400	-	F	F
Acetone Wet Sink Room Temperature	Photoresist	-	0	0	0	0	0	-	0	0	0	0	-	0	-	>44k	>39k
CF_4+CHF_3+He (90:30:120 sccm) Lam 590 Plasma 450W, 2.8T, gap=0.38cm, 13.56MHz	Silicon oxides	W	1900 1400 1900	2100 1500 2100	4700 2400 4800	W	4500	7300 3000 7300	6200 2500 7200	1800	1900	-	W	W	W	2200	2000
CF_4+CHF_3+He (90:30:120 sccm) Lam 590 Plasma 850W, 2.8T, gap=0.38cm, 13.56MHz	Silicon oxides	W	2200 2200 2700	1700 1700 2100	6000 2500 7600	W	6400 6000 6400	7400 5500 7400	6700 5000 6700	4200 4000 6800	3800	-	W	W	W	2600 2600 6700	2900 2900 7200
SF_6+He (13:21 sccm) Technics PE II-A Plasma 100W, 250mT, gap=2.6cm, 50kHz sq. wave	Silicon nitrides	300 300 1000	730 730 800	670 670 760	310	350	370	610	480 230 480	820	620 550 800	-	W	W	W	690 690 830	630
CF_4+CHF_3+He (10:5:10 sccm) Technics PE II-A Plasma 200W, 250mT, gap=2.6cm, 50kHz sq. wave	Silicon nitrides	1100	1900	W	730	710	730	W	900	1300	1100	-	W	W	W	690	600
SF_6+He (175:50 sccm) Lam 480 Plasma 150W, 375mT, gap=1.35cm, 13.56MHz	Thin silicon nitrides	W	6400	7000 2000 7000	300 220 400	W	280	530	540	1300 830 2300	870	-	W	W	W	1500 1300 1500	1400
SF_6+He (175:50 sccm) Lam 480 Plasma 250W, 375mT, gap=1.35cm, 13.56MHz	Thick silicon nitrides	W	8400	9200	800	W	770	1500	1200	2800 2100 4200	2100	-	W	W	W	3400 3100 3400	3100
SF_6 (25 sccm) Tegal Inline Plasma 701 125W, 200mT, 40°C	Thin silicon nitrides	W	1700	2800	1100 1100 1600	W	1100	1400	1400	2800 2800 2800	2300	-	W	W	W	3400 2900 3400	3100
CF_4+CHF_3+He (45:15:60 sccm) Tegal Inline Plasma 701 100W, 300mT, 13.56MHz	Si-rich silicon nitrides	W	350	360	320	W	320	530	450	760	600	-	W	W	W	400	360
Cl_2+He (180:400 sccm) Lam Rainbow 4420 Plasma 275W, 425mT, 40°C, gap=0.80cm, 13.56MHz	Silicon	W 5000 5000	5700 3400 6300	3200 3200 3700	8 8 380	-	60	230	140	560	530	W	W	-	-	3000 2400 3000	2700
HBr+Cl_2 (70:70 sccm) Lam Rainbow 4420 Plasma 200W, 300mT, 40°C, gap=0.80cm, 13.56MHz	Silicon	W	450 450 740	460	4 4 10	-	0	0	0	870	26	W	W	-	-	350 350 500	300
Cl_2+BCl_3+$CHCl_3$+N_2 (30:50:20:50 sccm) Lam 690 RIE 250W, 250mT, 60°C, 13.56MHz	Aluminum	W	4500	W	680	670	750	W	740	930	860	6000 1900 6400	W	-	-	6300 3700 6300	6300 3300 6100
SF_6 (80 sccm) Tegal Inline Plasma 701 200W, 150mT, 40°C, 13.56MHz	Tungsten	W	5800	5400	1200 2000 2000	W	1200	1800	1500	2600	2300 1900 2300	-	2800 2800 4000	W	W	2400 2400 4000	2400
O_2 (51 sccm) Technics PE II-A Plasma 50W, 300mT, gap=2.6cm, 50kHz sq. wave	Descumming photoresist	-	0	0	0	0	0	0	0	0	0	0	0	0	-	350	300
O_2 (51 sccm) Technics PE II-A Plasma 400W, 300mT, gap=2.6cm, 50kHz sq. wave	Ashing Photoresist	-	0	0	0	0	0	0	0	0	0	0	0	0	-	3400	3600
HF Vapor 1 cm over plastic dish Room temperature and pressure	Silicon oxides	-	0	0	660	W	780	2100	1500	10	19	A	0	A	-	P 0	P 0
XeF_2 Simple custom vacuum chamber Room temperature, 2.6 Torr	Silicon	4600 2900 100k	1900 1100 2500	1800 1100 2300	0	-	0	0	0	120 120 180	2 0 2	0	800 440 1000	290 50 380	-	0	0

Notation: - =test not performed; W=not performed, but known to *Work* (≥ 100 Å/min); F=not performed, but known to be *Fast* (≥ 10 kÅ/min);
P=some of film *Peeled* during etch or when rinsed; A=film was visibly *Attacked* and roughened.
Rates measured are rounded to two significant figures.
Etch areas are all of a 4-inch wafer for the transparent films and half of the wafer for single-crystal silicon and the metals.
Etch rates will vary with temperature and prior use of solution or plasma chamber, area of exposure of film, other materials present (e.g., photoresist), film impurities and microstructure, etc. *Some variation should be expected.*

Etch Rates for Micromachining and IC Processing (Å/min) v. 4.4 29 July 1996

U.C. Berkeley Microfabrication Laboratory / Berkeley Sensor & Actuator Center / Kirt R. Williams

The top etch rate was measured by the author with fresh solutions, clean chambers, etc.

The center and bottom values are the low and high etch rates observed by the author and others in the UCB Microlab using fresh and used solutions, clean and "dirty" chambers, etc.

ETCHANT EQUIPMENT CONDITIONS	TARGET MATERIAL	MATERIAL SC Si <100>	Poly n+	Poly undop	Wet Ox	Dry Ox	LTO undop	PSG unanl	PSG annld	Stoic Nitrid	Low-σ Nitrid	Al/ 2% Si	Sput Tung	Sput Ti	Sput Ti/W	OCG 820PR	Olin HntPR
Concentrated HF (49%) Wet Sink Room Temperature	Silicon oxides	-	0	-	23k 18k 23k	F	>14k	F	36k	140	52 30 52	42 0 42	<50	F	-	P 0	P 0
10:1 HF Sink 6 Room Temperature	Silicon oxides	-	7	0	230	230	340	15k	4700	11	3	2500 2500 12k	0	11k	<70	0	0
25:1 HF Sink 6 Room Temperature	Silicon oxides	-	0	0	97	95	150	W	1500	6	1	W	0	-	-	0	0
5:1 BHF Sink 8 Room Temperature	Silicon oxides	-	9	2	1000 900 1080	1000	1200	6800	4400 3500 4400	9	4 3 4	1400	<20 0.25 20	F	1000	0	0
Phosphoric Acid (85%) Sink 7 Heated Bath 160°C	Silicon nitrides	-	7	-	0.7	0.8	<1	37	24 9 24	28 28 42	19 19 42	9800	-	-	-	550	390
Silicon Etchant (126 HNO_3 : 60 H_2O : 5 NH_4F) Sink 8 Room Temperature	Silicon	1500	3100 1200 6000	1000	87	W	110	4000	1700	2	3	4000	130	3000	-	0	0
KOH (1 KOH:2 H_2O by weight) Sink 3 Heated Bath 80°C	<100> Silicon	14k	>10k	F	77 41 77	-	94	W	380	0	0	F	0	-	-	F	F
Aluminum Etchant Type A (16 H_3PO_4 : 1 HNO_3 : 1 HAc : 2 H_2O) Sink 8 Heated Bath 50°C	Alumnium	-	<10	<9	0	0	0	-	<10	0	2	6600 2600 6600	-	0	-	0	0
Titanium Etchant (20 H_2O : 1 H_2O_2 : 1 HF) Wet Sink Room Temperature	Titanium	-	12	-	120	W	W	W	2100	8	4	W	0 0 <10	8800	-	0	0
H_2O_2 (30%) Wet Sink Room Temperature	Tungsten	-	0	0	0	0	0	0	0	0	0	<20	190 190 1000	0	60 60 150	<2	0
Piranha (~50 H_2SO_4 : 1 H_2O_2) Sink 8 Heated Bath 120°C	Cleaning off metals and organics	-	0	0	0	0	0	-	0	0	0	1800	-	2400	-	F	F
Acetone Sink 5 Room Temperature	Photoresist	-	0	0	0	0	0	-	0	0	0	0	-	0	-	>44k	>39k
HF Vapor Wet sink--1 cm over plastic dish Room temperature and pressure	Silicon oxides	-	0	0	660	W	780	2100	1500	10	19	A	0	A	- -	P 0	P 0
XeF_2 Old lab--Simple custom vacuum chamber Room temperature, 2.6 Torr	Silicon	4600 2900 100k	1900 1100 2500	1800 1100 2300	0	-	0	0	0	120 120 180	2 0 2	0	800 440 1000	290 50 380	-	0	0
SF_6+He (175:50 sccm)--In THINSTD.RCP Lam 1--Lam 480 Plasma 150W, 375mT, gap=1.35cm, 13.56MHz	Thin silicon nitrides	W	6400	7000 2000 7000	300 220 400	W	280	530	540	1300 830 2300	870	-	W	W	W	1500 1300 1500	1400
SF_6+He (175:50 sccm)--In NITSTD1.RCP Lam 1--Lam 480 Plasma 250W, 375mT, gap=1.35cm, 13.56MHz	Thick silicon nitrides	W	8400	9200	800	W	770	1500	1200	2800 2100 4200	2100	-	W	W	W	3400 3100 3400	3100
CF_4+CHF_3+He (90:30:120 sccm) Lam 2--Lam 590 Plasma 450W, 2.8T, gap=0.38cm, 13.56MHz	Silicon oxides	W	1900 1400 1900	2100 1500 2100	4700 2400 4800	W	4500	7300 3000 7300	6200 2500 7200	1800	1900	-	W	W	W	2200	2000
CF_4+CHF_3+He (90:30:120 sccm)--In SIO2ET.RCP Lam 2--Lam 590 Plasma 850W, 2.8T, gap=0.38cm, 13.56MHz	Silicon oxides	W	2200 2200 2700	1700 1700 2100	6000 2500 7600	W	6400 6000 6400	7400 5500 7400	6700 5000 6700	4200 4000 6800	3800	-	W	W	W	2600 2600 6700	2900 2900 7200
Cl_2+BCl_3+$CHCl_3$+N_2 (30:50:20:50 sccm) Lam 3--Lam 690 RIE 250W, 250mT, 60°C, 13.56MHz	Aluminum	W	4500	W	680	670	750	W	740	930	860	6000 1900 6400	W	-	-	6300 3700 6300	6300 3300 6100
Cl_2+He (180:400 sccm)--In Recipes 400, 500, 550 Lam 4--Lam Rainbow 4420 Plasma 275W, 425mT, 40°C, gap=0.80cm, 13.56MHz	Silicon	W 5000 5000	5700 3400 6300	3200 3200 3700	8 8 380	-	60	230	140	560	530	W	W	-	-	3000 2400 3000	2700
HBr+Cl_2 (70:70 sccm)--In Recipes 500, 550 Lam 4--Lam Rainbow 4420 Plasma 200W, 300mT, 40°C, gap=0.80cm, 13.56MHz	Silicon	W	450 450 740	460	4 4 10	-	0	0	0	870	26	W	W	-	-	350 350 500	300
O_2 (51 sccm) Technics-c--Technics PE II-A Plasma 50W, 300mT, gap=2.6cm, 50kHz sq. wave	Descumming photoresist	-	0	0	0	0	0	0	0	0	0	0	0	0	-	350	300
O_2 (51 sccm) Technics-c--Technics PE II-A Plasma 400W, 300mT, gap=2.6cm, 50kHz sq. wave	Ashing Photoresist	-	0	0	0	0	0	0	0	0	0	0	0	0	-	3400	3600
SF_6+He (13:21 sccm) Technics-c--Technics PE II-A Plasma 100W, 250mT, gap=2.6cm, 50kHz sq. wave	Silicon nitrides	300 300 1000	730 730 800	670 670 760	310	350	370	610	480 230 480	820	620 550 800	-	W	W	W	690 690 830	630
CF_4+CHF_3+He (10:5:10 sccm) Technics-c--Technics PE II-A Plasma 200W, 250mT, gap=2.6cm, 50kHz sq. wave	Silicon nitrides	1100	1900	W	730	710	730	W	900	1300	1100	-	W	W	W	690	600
SF_6 (80 sccm) Tegal--Tegal Inline Plasma 701 200W, 150mT, 40°C, 13.56MHz	Tungsten	W	5800	5400	1200 2000 2000	W	1200	1800	1500	2600	2300 1900 2300	-	2800 2800 4000	W	W	2400 2400 4000	2400
SF_6 (25 sccm) Tegal--Tegal Inline Plasma 701 125W, 200mT, 40°C	Thin silicon nitrides	W	1700	2800	1100 1100 1600	W	1100	1400	1400	2800 2800 2800	2300	-	W	W	W	3400 2900 3400	3100
CF_4+CHF_3+He (45:15:60 sccm) Tegal--Tegal Inline Plasma 701 100W, 300mT, 13.56MHz	Si-rich silicon nitrides	W	350	360	320	W	320	530	450	760	600	-	W	W	W	400	360

Notation: - =test not performed; W=not performed, but known to Work (≥ 100 Å/min); F=not performed, but known to be Fast (≥ 10 kÅ/min);
P=some of film Peeled during etch or when rinsed; A=film was visibly Attacked and roughened.
Rates measured are rounded to two significant figures.
Etch areas are all of a 4-inch wafer for the transparent films and half of the wafer for single-crystal silicon and the metals.
Etch rates will vary with temperature and prior use of solution or plasma chamber, area of exposure of film, other materials present (e.g., photoresist), film impurities and microstructure, etc. *Some variation should be expected!*